ISSN : 0019-5693

INDIAN JOURNAL
OF
THEORETICAL PHYSICS

VOLUME 67 NOS. 1,2

JANUARY, 2019 – JUNE, 2019

Published by the
CALCUTTA INSTITUTE OF THEORETICAL PHYSICS
(Formerly, INSTITUTE OF THEORETICAL PHYSICS)
"BIGNAN KUTIR"
4/1, MOHAN BAGAN LANE, KOLKATA-700004

(Peer-reviewed Journal)

ISSN : 0019-5693

INDIAN JOURNAL
OF
THEORETICAL PHYSICS

[Founder President : Late Prof. K. C. Kar, D. Sc.]

VOLUME 67 **NOS. 1,2**

JANUARY, 2019 – JUNE, 2019

INDIAN JOURNAL
OF
THEORETICAL PHYSICS

"BIGNAN KUTIR"
4/1, MOHAN BAGAN LANE, KOLKATA-70004, INDIA

SUBSCRIPTION RATE

INDIA : For Library (Institute)

₹ 1500.00 for each volume

FOREIGN : $ 350 for each volume

Drafts, Orders, Enquiries & Claim for Non-Receipt of Journal should be sent to :

CALCUTTA INSTITUTE OF THEORETICAL PHYSICS
(Formerly, INSTITUTE OF THEORETICAL PHYSICS)
"BIGNAN KUTIR"
4/1, MOHAN BAGAN LANE, KOLKATA-700004, India

C O N T E N T S

INDIAN JOURNAL OF THEORETICAL PHYSICS, VOL 67, NOS. 1 & 2, 2019

Scattering of e^+-Li^{2+}-ion

Mukesh Kumar Sinha[1] Randhir Kumar[2] and Tarun Kumar Dey[3]

[1]Department of Physics, L.N.J.P.Institute of Technology,
Chapra - 841302 (Bihar)
E-mail : mukeshphysics11@gmail.com

[2]Department of Physics, J. P. University, Chapra
E-mail: krandhir782@gmail.com

[3]Post Graduate Department of Physics, L.S.College,
Muzaffarpur-842001 (Bihar)
E-mail : tkdeyphy@gmail.com

[Abstract : The differential and total cross sections for elastic scattering of positron by Li^{2+} ion in the intermediate and high energy ranges have been calculated by using distorted wave method without polarisation potential (DCSWP) and with polarisation potential (DCSPP). The impact of polarisation effect has been analyzed. Perturbing potential is weaker than that of Born approximation. Phase shifts for $e^+ - Li^{2+}$ scattering are calculated. The results are compared with available theoretical data.]

Key words : Elastic scattering, differential cross section, distorted wave method, polarisation potential, phase shift.

1 Introduction

The positron ion scattering help us to finding the behavior of the positron in presence of the long-range Coulomb potential and the attractive polarisation potential in the energy range $100ev - 400\,ev$.

Burgess, Hummer and Tully[1] have investigated electron-helium ion scattering by Coulomb Born Oppenheimer approximation and used partial wave method. Mitra and Sil[2] have observed that partial wave method is not suitable at high energy.

Mitra and Sil[2] have evaluated Coulomb-Born and Coulomb Born Oppenheimer cross-sections for $1s - 2s$ excitation of hydrogen like ions by electron impact, without using partial wave method whereas the distorted wave polarised orbital method is used by Mc. Dowell[3.4] with due success.

In intermediate and high energy ranges, we have used the variant of distorted wave method that accounts for the effect of continuum and effect of higher excited states. In this approach, we included a part of Coulomb potential in continuum wave function in the initial channel. The nucleus of the target atom has been taken as screened nucleus. The dipole polarisation potential has been included which accounts for excited states partially. This approach has been used in the scattering of positrons by complex atoms with due success by Verma and Roy[5].

2 Theory:

The Hamiltonian H for positron-lithium ion can be expressed as :

$$H = \left[-\frac{1}{2}\nabla_{r_1}^2 - \frac{1}{2}\nabla_{r_2}^2 - \frac{1}{r_1} \right] + \left[\frac{1}{r_2} - \frac{1}{r_{12}} \right] \qquad \text{... (1)}$$

In centre-of-mass reference frame, $\vec{r_1}$ and $\vec{r_2}$ are the position vectors of the atomic electron and the incident positron with respect to the screened nucleus of the target atom. $\nabla^2_{r_1}$ and $\nabla^2_{r_2}$ are the kinetic energy operators. Atomic units are used throughout.

The Hamiltonian H is partitioned and expressed as :

$$H = H_1 + W \quad \text{... (2)}$$

with

$$H_1 = H_0 + U \quad \text{... (3)}$$

where

$$U = \delta / r_2 \quad \text{... (4)}$$

$$W = \frac{(1-\delta)}{r_2} - \frac{1}{r_{12}} \quad \text{... (5)}$$

δ = screening parameter.

and H_0 = Free Hamiltonian

The function ϕ_r, χ_r and ψ_r satisfy the following Schrodinger equations with Hamiltonian H_0, H_1 and H respectively.

$$\left.\begin{aligned} H_0\phi_r &= E_r\phi_r \\ H_1\chi_r &= E_r\chi_r \\ H\psi_r &= E_r\psi_r \end{aligned}\right\} \quad \text{... (6)}$$

Where, E_r is the total energy of the system.

Let the system move from initial bound state $|i\rangle$ with momentum $\overline{K}_i$ to the final state $|f\rangle$ with momentum $\overline{K}_f$. Assuming, W to be a weak potential.

T-matrix elements can be expressed as :-

$$T_{i\to f} = \left\langle \phi_f \mid V \mid \psi_i^{(+)} \right\rangle \quad \text{... (7)}$$

where

$$V = \frac{1}{r_2} - \frac{1}{r_{12}} \quad \text{... (8)}$$

Here, $\psi_i^{(+)}$ can be expanded with respect to H_1 as

$$\psi_i^{(+)} = \sum_{n=0}^{\infty} \left(G^{(+)} W \right)^n \chi_i^{(+)} \quad \text{... (9)}$$

where, $G^{(+)}$ is the Green function for H_1.

It would not be crude approximation to retain the first order term in the above expression.

$$T_{i\to f} = \left\langle \phi_f \mid V \mid \chi_i^{(+)} \right\rangle \quad \text{... (10)}$$

In atomic unit, differential cross section is expressed as :

$$\frac{d\sigma}{d\Omega} = \frac{\mu^2}{4\pi^2} \frac{K_f}{K_i} \left| T \right|^2 \quad \text{... (11)}$$

and total cross-section is obtained by integrating the above expression :

$$\sigma = \int \left(\frac{d\sigma}{d\Omega} \right) d\Omega \quad \text{... (12)}$$

Here, wave functions have been taken in the following forms :

$$\phi_r = \exp\left(i\bar{K}.\bar{r}_2 \right) \phi_{nlm}\left(\bar{r}_1 \right) \quad \text{... (13)}$$

$$\chi_i^{(+)} = \Gamma\left(1 + ia\right) \exp\left(i\bar{K}.\bar{r}_2 - \frac{\pi a}{2} \right) {}_1F_1\left(-ia; 1; iK_i r_2 - i\bar{K}_i.\bar{r}_2 \right) \phi_{nlm}\left(\bar{r}_1 \right) \quad \text{... (14)}$$

where,

$$a = \delta / K \quad \text{... (15)}$$

Here, $\overline{K}$ is the momentum for the direct channel in which distortion is introduced. The screening parameter δ is evaluated by the method of Junker[6].

This method takes the part of Coulomb potential in incident continuum wave function. Physically, the effect of continuum is taken into account partially.

The radial part of wave function for lithium ion is expressed as :

$$\varphi_n(r) = \sum_i a_i r^{n-1} \exp(-b_i r) \quad \text{... (16)}$$

For ground state,

$$n = 1; a_1 = \frac{Z^{3/2}}{\sqrt{\pi}}; b_1 = Z$$

For 2s state,

$$n = 2; a_1 = \frac{Z^{3/2}}{2\sqrt{2\pi}}; b_1 = \frac{Z}{2} \quad \text{... (17)}$$

$$a_2 = -\left(\frac{Z}{2}\right) a_1; b_2 = \frac{Z}{2}$$

Now, T-matrix can be expressed in the following form :

$$T_{i\to f} = MF' \left[N_1 \frac{\partial I}{\partial \lambda} + N_2 \frac{\partial^2 I}{\partial \lambda^2} \right] \quad \text{... (18)}$$

In above expression :

$$\left.\begin{aligned} MF' &= \Gamma(1+ia)\exp\left(-\frac{\pi a}{2}\right) \\ \lambda &= \frac{3Z}{2} \\ N_1 &= -\frac{4\pi Z^3}{2\sqrt{2\pi}}\left(\frac{2Z}{\lambda^3}-\frac{1}{\lambda^2}\right) \\ N_2 &= \frac{4\pi Z^3}{2\sqrt{2\pi}}\left(\frac{Z/2}{\lambda^2}\right) \end{aligned}\right\} \quad \text{... (19)}$$

$$I = \iint \exp\left(i\bar{q}.\bar{r}_2\right)\,{}_1F_1\left(-ia;1;iK_i r_2 - i\bar{K}_i.\bar{r}_2\right)\frac{e^{-\lambda r_1}}{r_{12}}d\bar{r}_1 d\bar{r}_2 \quad \text{... (20)}$$

where,

$\bar{q} = \bar{K}_i - \bar{K}_f$

Using Nordsieck[7] method, the integrals involved in differential cross-sections are evaluated.

Polarisation potential :

The polarisation potential has been taken in the following form -

$$V_p(x) = -\frac{9}{4\pi^2}\left[1-e^{-2x}\left(1+2x+2x^2+\frac{4}{3}x^3+\frac{2}{3}x^4+\frac{4}{27}x^5\right)\right] \quad \text{... (21)}$$

where, $x = zr_2$

The differential cross sections are calculated with polarization potential (DCSPP) and without polarization potential (DCSWP) to analyse the impact of interaction on scattering of positron. The total cross-sections are calculated using the equ^{n}(12).

Phase shifts :

In the case of positron scattering, the radial wave function satisfy the following equations.

$$\left[\frac{d^2}{dx^2} - \frac{l(l+1)}{x^2} + k^2\right] g_l(x) = 0 \qquad \text{... (22)}$$

$$\left[\frac{d^2}{dx^2} - \frac{l(l+1)}{x^2} - V(x) + k^2\right] u_l(x) = 0 \qquad \text{... (23)}$$

where, x = co-ordinate of the incident positron,

$V(x)$ = sum of static potential and polarisation potential,

$g_l(x)$ and $u_l(x)$ = components of radial wave function such that $g_l(0) = 0$, $u_l(0) = 0$ at $x = 0$.

In the intermediate and high energy ranges, the potential has been taken to be weak potential and approximate solutions of above differential equations have been obtained and phase shifts have been evaluated. Precautions are taken to avoid divergence. The evaluated phase shifts are compared with available theoretical data.

3 Results and Discussion :

Differential Cross-sections :

The differential cross-sections have been calculated by using distorted wave method without Polarisation Potential and with polarisation potential are represented by curve A and curve B respectively in the intermediate and high energy range.

At all energy ranges, the curve B lies below the curve A. This shows the impact of polarisation interaction.

At 100 eV, the curve B lies below the curve A at all angles. This displays the effect of polarisation potential as reduction in differential cross-section. Both the curves have tendency of merging together at nearly 0^0 scattering angle. This is expected. This is clear evidence that the present results are justified and present approach is suitable one.

At 200 eV, the reduction in differential cross-sections is larger than the same at 100 eV at 5^0 scattering angle. This shows the enhancement of effect of polarisation interaction near the forward direction. At larger scattering angle the relative difference between DCSPP and DCSWP is more. Similar feature is observed at 100 eV.

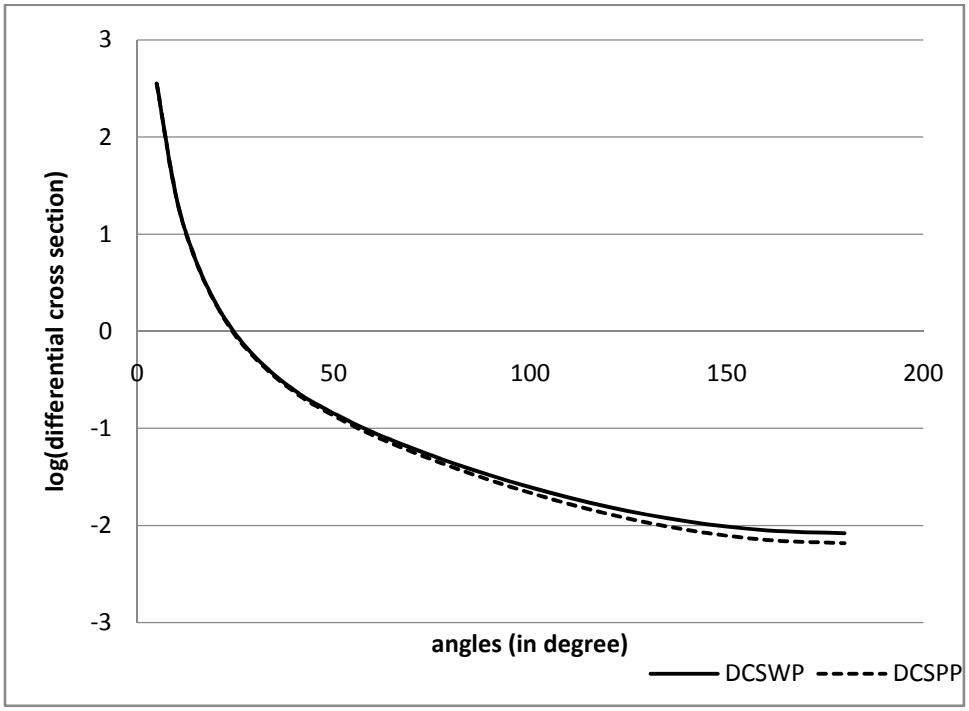

Fig. 1
$e^+ - Li^{2+}$scattering at energy 100ev

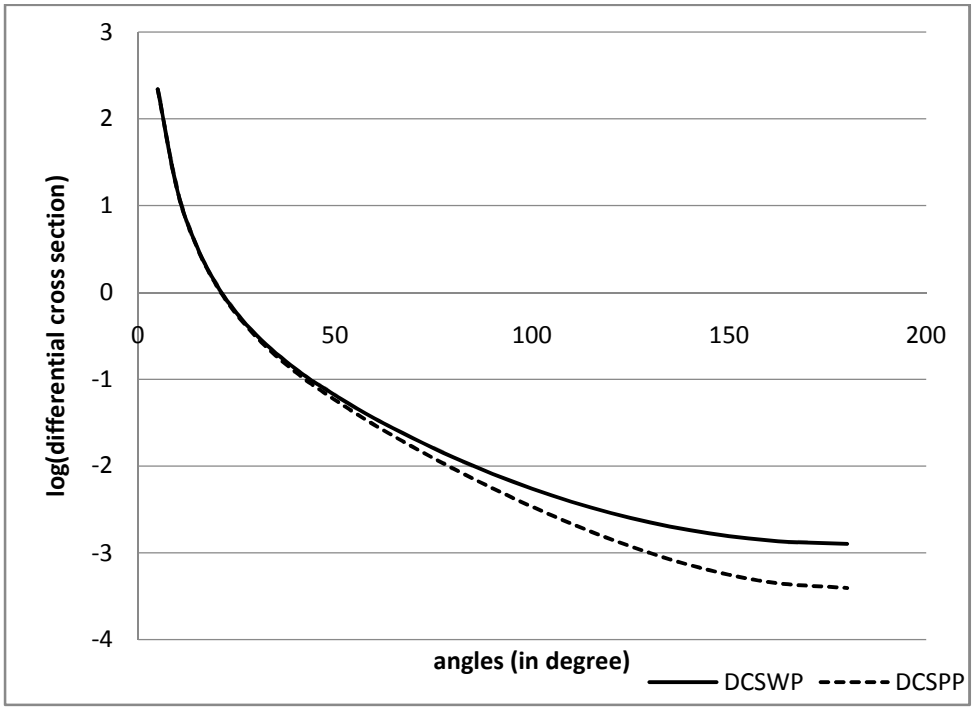

Fig. 2
$e^+ - Li^{2+}$scattering at energy 200ev

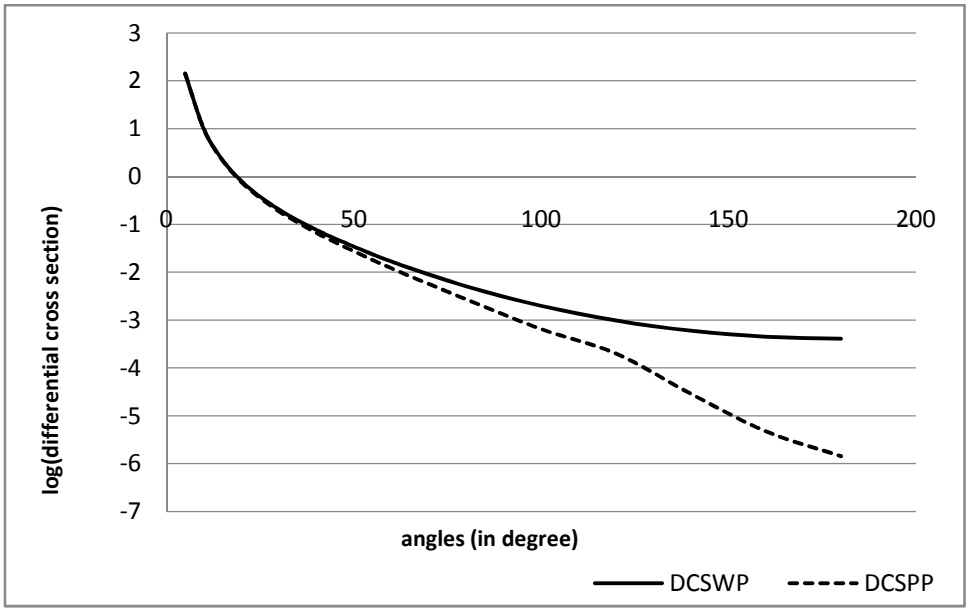

Fig. 3
$e^+ - Li^{2+}$ scattering at energy 300ev

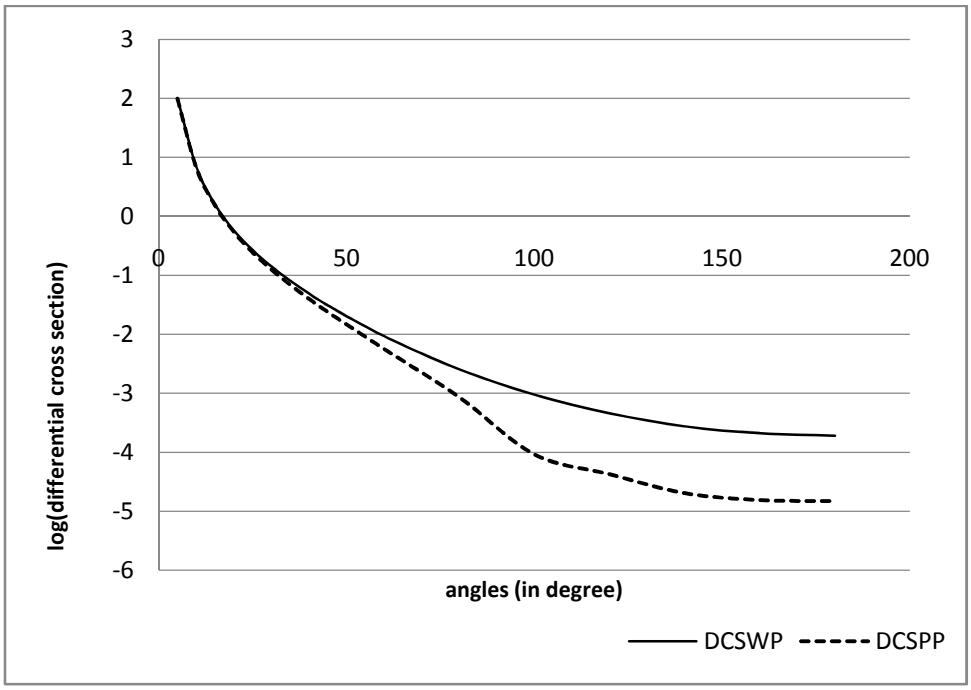

Fig. 4
$e^+ - Li^{2+}$ scattering at energy 400ev
A - DCSWP
B - DCSPP

At 300 eV and 400 eV, apart from features mentioned above DCSPP is observed to have larger values than corresponding values of DCSWP at larger scattering angles. This may be due to effect of adiabatic polarisation. Here, at smaller scattering angles the values of DCSPP are less than corresponding values of DCSWP.

In present method, continuum distorted wave functions have been used in the state wave function. It takes into account the effect of continuum on elastic channel. Moreover, in this method, perturbing potential is weaker than that of Born approximation. It is expected that the results obtained by using the present method contain higher order terms. The theoretical soundness of the present theory is well conceived.

Phase shifts :

Table - 1

s-wave phase shifts (rad) for e^+-Li^{2+} elastic scattering -			
Energy (in eV)	η_P	η_{TL}	η_C
18.324	0.10 (-2)	0.11 (-2)	0.10 (-2)
20.512	0.11 (-2)	0.13 (-2)	0.12 (-2)
23.293	0.16 (-2)	0.17 (-2)	0.15 (-2)
34.647	0.21 (-2)	0.25 (-2)	0.19 (-2)
41.360	0.18 (-2)	0.23 (-2)	0.14 (-2)
48.057	0.17 (-2)	0.14 (-2)	0.20 (-2)
56.787	-0.21 (-2)	-0.60 (-2)	-0.22 (-2)
66.219	-0.48 (-2)	-0.37 (-2)	-0.59 (-2)
78.823	-1.01 (-2)	-0.90 (-2)	-1.19 (-2)

Table - 2

p-wave phase shifts (rad) for e^+-Li^{2+} elastic scattering -			
Energy (in eV)	η_P	η_{TL}	η_C
18.324	0.62 (-3)	0.70 (-3)	0.60 (-3)
20.512	0.81 (-3)	0.80 (-3)	0.80 (-3)
23.293	0.11 (-3)	0.10 (-3)	0.10 (-3)
34.647	0.20 (-2)	0.21 (-2)	0.19 (-2)
41.360	0.24 (-2)	0.25 (-2)	0.23 (-2)
48.057	0.28 (-2)	0.30 (-2)	0.26 (-2)
56.788	0.29 (-2)	0.32 (-2)	0.27 (-2)
66.219	0.30 (-2)	0.33 (-2)	0.26 (-2)
78.823	0.25 (-2)	0.29 (-2)	0.21 (-2)

Table - 3

d-wave phase shifts (rad) for e^+-Li^{2+} elastic scattering -			
Energy (in eV)	η_P	η_{TL}	η_C
18.324	0.34 (-3)	0.40 (-3)	0.30 (-3)
20.512	0.39 (-3)	0.40 (-3)	0.40 (-3)
23.293	0.48 (-3)	0.50 (-3)	0.50 (-3)
34.647	0.10 (-2)	0.10 (-2)	0.10 (-2)
41.360	0.11 (-2)	0.13 (-2)	0.13 (-2)
48.057	0.16 (-2)	0.17 (-2)	0.15 (-2)
56.787	0.18 (-2)	0.20 (-2)	0.18 (-2)
66.219	0.22 (-2)	0.24 (-2)	0.21 (-2)
78.823	0.26 (-2)	0.27 (-2)	0.24 (-2)

η_P - Present value of phase shifts.

η_{TL} - Phase shift with the potential of Temkin-Lamkin.

η_C - Phase shift with potential of Callaway.

The table-1, Table-2 and Table-3 contain the values of phase shifts predicted by Khan, Mazumdar and Ghose[8] by using two variants of polarised orbital method. η_C and η_{TL} are the phase shifts evaluated by above investigators with potential of Callaway[9] and the potential of Temkin and Lamkin[10] respectively.

Our present set of results for s-wave, p-wave and d-wave phase shifts show good agreement with corresponding values of η_C and slight difference with η_{TL}. This slight difference may be only due to diabetic potential which is repulsive in nature and adds to the repulsive static potential. The observed agreement establishes the fact that present approach is good and can be further used in theoretical investigations of positron ion-scattering.

References

1. Burgess, A., Hummer, D.G. and Tully, J.A. 1970, Phil. Trans. R. Soc. London **A, 266**, 225.
2. Mitra C. and Sil N.C., Phys. Rev**. A. 14**, 1009 (1976).
3. Mc. Dowell MRC, Morgan I.A. and Myerscough V.P., 1975, J.Phys. B: At. Mol. Phys. **8,** 1053-72.
4. Sinha Nidhi, Singh Suvam and Antony Bobby, 2018. J. Phys. B : At. Mol. opt. Phys. **51**, 015204.
5. Verma, P.K. and Roy, D.N., Ind. J. Phys**. 68B** (5) (1994) P.389-397.
6. Junker B.R., Phys. Rev. **A. 2** : 1552 (1975).
7. A. Nordsieck, Phys. Rev. **A. 93**, 785 (1954).
8. Khan P., Mazumdar P.S. and Ghosh A.S., Z.Phys**. A. 318**, 19 (1984).
9. Callaway J. Comput. Phys. Commun. **6**, 265 (1974).
10. Temkin J. and Lamkin J.C., Phys. Rev. **121**, 788 (1961).

———

INDIAN JOURNAL OF THEORETICAL PHYSICS, VOL 67, NOS. 1 & 2, 2019

Role of Photonics in Building Light Energy Conversion Devices

Somnath Paul, Ishani Mitra, Tapan Ganguly*

School of Laser Science and Engineering, Jadavpur University,

Jadavpur, Kolkata 700032, India

Email: tapcla@rediffmail.com

[Abstract : Our present investigations by steady state and time resolved spectroscopic techniques demonstrate that when the short-chain dyads combine with nanoparticles of noble metals such as silver, gold and gold/silver coreshell nanocomposite systems or carbon quantum dots as well as graphenes, they primarily exhibit efficient artificial light energy conversion materials or nanocomposite devices.]

Keywords: time resolved spectroscopy, nanocomposite dyad, trans-cis conversion, charge separation, charge recombination, energy storage

1. Introduction

The photonics in energy conversion process plays significant role. The amount of energy received by our earth from the sun in just one hour is of significantly larger amount than the yearly consumption need of our earth. The enormous energy of the sun can be utilized in the three

*author to whom all correspondences should be addressed

main ways. They are (1) conversion of sunlight to electrical power, (2) conversion of sunlight to thermal power and (3) conversion of sunlight directly to fuels. Most solar cells work on the basis of conversion of sunlight into electricity using the photovoltaic (PV) effect . The most important commercially available PV materials systems today are based on inorganic semiconductors. The majority of solar modules are based on silicon, which is the second most abundant material in the earth and the efficiency of silicon solar cell is nearly 25.6%. Photonics plays an important role in Si-based solar cells and modules since it is an indirect band gap semiconductor and hence has a relatively long absorption depth across the solar spectrum. Most importantly, light-trapping structures must be fashioned on the front surface of the wafers to ensure that long wavelength light is adequately trapped within the solar cell and is not lost from reflection at the back contact.

In recent times, low-cost dye-sensitized solar cells (DSSCs) have attracted much attention with their relatively high energy conversion efficiencies[1–10]. One of the major advantages of DSSC is that by varying the combinations of the dyes and semiconductor materials the cell performance can be improved[9]. Many attempts have been made to synthesize alternative molecular dyes to extend the spectral response but the low absorption cross section and instability under strong illumination inhibited significant efficiency increase. Our research group[8] used a novel concept to increase the solar cell performances by using mixture of dyes compare to single dye and found that cell performance enhanced in case of dye mixtures with ZnO and TiO_2 nanomaterials working as electrodes in a simple device configuration. Only the difference is that instead of liquid electrolyte we have used PEDOT: PSS layer as a hole

transporting medium. In a similar type of cell configuration Jiang et al.[11] had used Poly (4-vinylphenyloxymethyltriphenylamine) as hole transport material for N-719 dye sensitized TiO_2 solar cell. Though in the liquid electrolyte based DSSCs, the photon-to-current conversion efficiency is much greater than that of DSSCs using no electrolyte, but our experimental observations showed[8] the enhancement of absorption properties of dye mixture which may be useful in designing solar cell having high efficiency. Dye sensitized solar cells have advantages over electrolyte-solar cells as the former possess high thermal stability and there is no possibility of leakage of electrolyte due to accidental breakage of substrate.

Our another attempts to build some novel solar cells by adsorbing a short-chain dyad on the nanosurfaces of TiO_2 nanoparticles where TiO_2 does not act as an electron acceptor but it simply protects the charge-separated species formed within the dyad[12].

Very recently our group is now involved to investigate the quantum dot sensitized solar cells where it is expected that the efficiency of solar cells should be enhanced considerably relative to dye sensitized solar cells. Thus various attempts are being made to convert solar energy to electrical (solar cells) and other useful energy (storage devices by using short-chain organic dyads).

Modern researches on photoswitchable dyads are of great importance due to their applications in designing solar cells, optical data storage, molecular electronics, artificial light energy converters etc. To understand the nature of the mechanisms of the charge separation and energy destructive charge recombination processes within these dyads the time resolved spectroscopy measurements and theoretical

computations on a novel synthesized dyad MNTMA(where the electron donor methoxy naphthalene being connected with an acceptor p-methoxy acetophenone by a short chain), have been studied. Earlier experimental evidences demonstrate that various short-chain dyad systems possess two types of conformers in the excited state though experimental evidences infer in favor of only one conformer in ground state [13, 14].

Our recent investigations by steady state and time resolved spectroscopic techniques demonstrate that when the short-chain dyads combine with nanoparticles of noble metals such as silver, gold and gold/silver coreshell nanocomposite systems or carbon quantum dots as well as graphenes, they exhibit efficient artificial light energy conversion materials or nanocomposite devices.

2. Experimental

The methods of synthesis with characterization of the short chain dyads and nanomaterials are described elsewhere[15].

$UV-$vis absorption and steady state fluorescence emission spectra of dilute solutions $(10^{-4} - 10^{-6}M)$ of the dyad were recorded at the ambient temperature (296 K) using 1 cm path length rectangular quartz cells by means of an $UV-$vis absorption spectrophotometer (JASCO$UV-V$is absorption spectrometer, Model: V-630) and JASCO spectrofluorimeter Model: 8200) respectively.

Fluorescence lifetimes were determined by using a time correlated single photon-counting (TCSPC) technique with the model FLUOROLOG TCSPC HORIBA JOBIN YVON using nanosecond laser of 375 nm (Horiba scientific, DD-375L) as excitation source profile. The quality of fit is assessed over the entire decay, including the rising edge,

and tested with a plot of weighted residuals and other statistical parameters e.g., the reduced $\chi 2$ and the Durbin–Watson (DW) parameters. *The femtosecond-resolved fluorescence decays* were measured by using a femtosecond upconversion setup (FOG100, CDP). The samples were excited at 375 nm using thesecond harmonic of a mode-locked Ti-sapphire laser with an 80 MHz repetition rate (Tsunami, Spectra Physics),pumped by 10 W Millennia (Spectra Physics).

Nanosecond laser flash photolysis (Applied Photophysics) containing Nd:YAG laser (Lab series, Model Lab 150, Spectra physics) was used to measure transient absorption decays.

All the solutions prepared for room temperature measurements were deoxygenated by purging with an argon gas stream for 30 min.

3. Discussion

Our present investigations have been primarily involved to design various light energy conversion nanocomposite devices where the short-chain organic dyads being adsorbed within the surface of noble nanometals especially nanomatals spherical gold, gold nanostar (GNS) and spherical silver behave as promising artificial light energy conversion and energy storage devices. From these investigations, done by the steady state and time resolved spectroscopic techniques, the adsorbed dyads were observed to possess mostly elongated or extended conformations in the excited state though conversion of extended to folded geometry was found in case of the pristine dyad only. As this elongated nature facilitates the charge separation rate inhibiting the energy destructive charge recombination processes, the nanocomposite dyads appear to be better light enery conversion devices than its pristine

form. From our investigation it is revealed that use of metal-semiconductor or metal-metal core-shell nanoparticles may provide new ways to modulate charge recombination processes in light energy conversion devices. A schematic diagram (Scheme)was proposed to show the possible mechanisms of charge separation and energy destructive charge recombination rate processes for a pristine dyad (folded conformation in the excited state) and nanocomposite dyads where the dyad adsorbs on the nanosurface of Ag nanoparticles and Ag shell of Au@Ag core-shell system. Interestingly in both the cases though the dyad adsorbs on the nanosurface of Ag, but it exhibits the different conformations. In first case, as shown in the scheme 1, folded conformation of the excited state dyad prevails relative to its elongated forms but in the latter case the reverse situation occurs where the elongated conformation of the dyad dominates.

Apart from noble nanometals and their core-shell systems, carbon quantum dots (CQD) and its ethylenediamine (EDA) functionalized CQD (NCQD) were also used to adsorb novel synthesized short-chain dyads on its nanosurface to retain trans-form or elongated nature in order to minimize energy destructive charge recombination rates 15. On comparing the experimental results of the dyad–gold nanocomposites with dyad-CQD (or NCQD), it is clearly observed[15] that in the former case (using especially pop-corn or star-shaped gold nanoparticles) maximum 60% of the ground state trans conformers could be retained in the excited state whereas more than 80% (as evidenced from time resolved measurements) trans structure of the ground state dyad could be protected in the environment of CQD (or NCQD) even on

photoexcitation. As trans- conformers facilitate the formation of longer lived charge- separated species i.e., slower energy destructive charge recombination rates, the dyad-CQD (or NCQD) nanocomposites appear to be relatively better light energy converter or energy-storage systems.

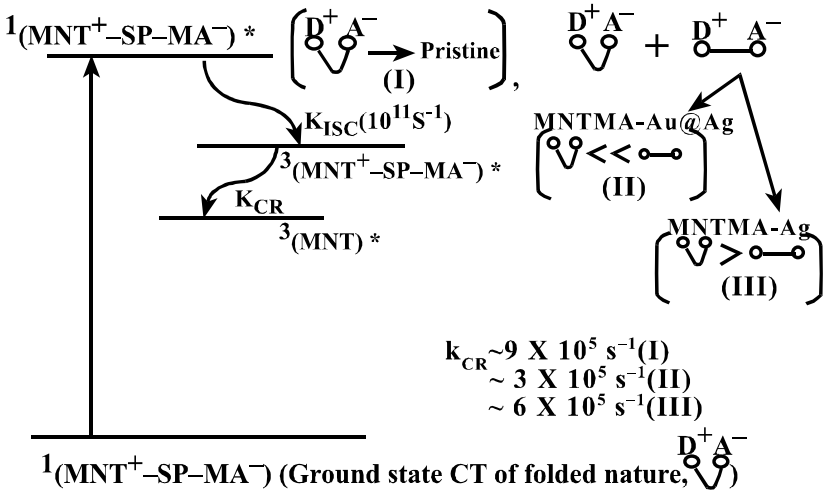

The hindrance of trans-cis conversion or stability of trans-structured species of nanocomposite dyad on photoexcitation appears to be due to joint effects of surface coverage and surface trap effects, the later process appears to be dominant. However, the exact mechanisms are yet to be explored. Possibility of increase of steric strain within the trans structured dyad has been hinted for its stable conformation. The nanocomposite dyads seemingly act as more efficient light energy converters relative to its pristine form

Scheme The possible mechanisms of charge separation and energy destructive charge recombination rate processes for a pristine dyad and nanocomposite dyads.

Further investigations are underway with different short-chain dyads being adsorbed on Graphene oxide (GO) and reduced Graphene oxide (RGO) to examine whether the dyad being combined with the GO or RGO would serve as better artificial light energy converters than dyad-CQD or NCQD. Some preliminary investigations demonstrate that dyad-CQD appears to be more effective light energy converter which could serve as better energy storage. Further investigations are now under progress.

The retention of trans-form (elongated conformation) will help to slow down energy wasting charge recombination processes within nanocomposite dyads and may serve as better candidate for artificial light energy conversion systems relative to its pristine form. Thus the short-chain dyads being combined with the GO or RGO would serve as better artificial light energy converters and charge storage systems relative to its pristine one. From time resolved spectroscopic measurements it could be hinted that relatively stable trans-conformer in the excited state in case of the nanocomposite system of an organic short-chain dyad -GO (or RGO) in comparison to the pristine form may arise from the surface trap effect.

This electron transfer (ET) possibility within the redox components (donor and acceptor moieties) could be examined by using Rehm-Weller relaltion[16,17] .

$$\Delta G0 = E^{OX}{}_{1/2}(D/D+) - ERED_{1/2}(A-/A) - E_{00}{}^{*} \quad \ldots (1)$$

where the symbols have their usual meanings. From the electrochemical measurements the half-wave oxidation and reduction potentials were determined.

The potential parameters were determined to be ($EOX_{1/2}(D/D+) \sim +1.85\,V, ERED_{1/2}(A-/A) \sim -1.02\,V$) and E^* is chosen at 3.35 eV (370 nm). The driving energy, ΔG^0value was computed to be $-0.48\ eV$. This shows there is a possibility from thermodynamic point of view the occurrence of electron transfer reactions within the dyad in the excited singlet state. Now,since the back ET for formation of the ground state is also largely possible from charge recombination mechanism as evidenced from large negative value ($-2.87\ eV$) of $\Delta G_b(G)$, estimated from the relation,

$\Delta Gb(G) = -E\,(D/D+) + E\,(A-/A)$ ("G" for ground state) ... (2)

it appears that the formation of ground state dyad through charge recombination would be largely facilitated in case of pristine dyads (which have only $c$is structure in the excited state). The situation would be less favored in case of trans-structure of the excited dyad (due to elongated form, the redox partners will be far apart). Thus it seemingly indicates that the yield of charge separated states would be lower in case of pristine dyad and due to stability the charge separated yield will become larger in case of the nanocomposite dyads where the dyad combines with GO and RGO.

Electron transfer reactions are the radiationless transitions and the rate defined in a golden rule type expression in which the rate is given as the product of an electronic matrix element squared H_{DA}^2 and Franck-Condon weighted density (FCWD) of states.The rate constant of electron transfer under nonadiabatic condition is given by,

$k_{CS} = \frac{2\pi}{\hbar}\, l\, H_{DA} l^2\, FCWD$ ... (3)

In semiclassical treatment approximation the equn (3) could be rewritten as

$$k_{cs} = \left(\frac{\pi}{\hbar^2 \lambda kT}\right)^{\frac{1}{2}} 1H_{DA}1^2 \sum_{0}^{\infty} \left(\frac{e^{-s}S^{v}}{v!}\right) \exp\{-[\Delta G^0 + \lambda_3 + \upsilon h\upsilon)^2 /4\lambda_3 kT]\} \quad \ldots (4)$$

The above expression (4) represents the overall rate of electron transfer reactions from the donor to the different vibrational energy levels of the acceptor, λs denotes the solvent reorganization energy parameter. The summation term is the nuclear factor which gives the dependencies of electron transfer on exergonicity, - ΔG^0.

From the above expressions (3) or (4) it is apparent that as H_{DA} is of higher value in case of pristine dyad (in this case excited singlet formations of cis-configuration facilitate),so charge-separated yield would be relatively lower than the situation when trans-form will dominate in the case of nanocomposite systems where the dyad combines with GO or RGO. In the later case lesser H_{DA} value will slow down the energy wasting charge recombination process enhancing the charge-separated yield.

As GO (or RGO) possesses considerable technological applications[18], apart from its current research interests, in serving our society our undergoing project is now to build organic supercapacitors and related artificial light energy conversion devices (storage components) with GO and RGO being combined with various novel synthesized short-chain organic dyads. Our primary goal is to design highly efficient supercapacitors and energy storage systems which

should be of physically and chemically stable, biocompatible, biosafe and cost-effective.

Acknowledgments

TG gratefully acknowledges the University grant commission (UGC), New Delhi, India for awarding Emeritus fellowship and contingency grant (F.6-6/2014-15/EMERITUS-2014-15-GEN-3976) for research purposes. SP expresses his deep sense of gratitude to the authority of Jadavpur University for providing JU-RUSA 2.0 Post-Doctoral Fellowship.

References

1. McDonald S. A. et al. Nat. Mater. **2005**, 4, 138
2. Katagiri H. et al., Thin Solid Films **2009**, 517, 2455
3. Jeong S. et al., Energy Environ. Sci.**2012,**5, 7539
4. Krebs F. C. et al., Nanoscale**2010,** 2, 873
5. O'Regan B. and Graetzel M., Nature**1991,**353, 737
6. Yu Q. et al., Nano ACS **2010,**4, 6032.
7. Yella A. et al., Science**2011,**334, 629
8. Bhattacharya S., Mandal G, Dutta M, Basak D. and **Ganguly*T,**J Nanosci Nanotech **2011,** 11, 7735
9. Kafafi Z. H. et al., Photonics J for energy 2015, 5, 050997
10. Kim Y., Cook S., Tuladhar S. M., Choulis S. A., Nelson J., Durrant J. R., D. Bradley D. C., Giles M., McCulloch I., Ha C.-S., and Ree M., Nature Mater.**2006,**5, 197.
11. Jiang K. J., Sun Y. L., Shao K. F., Wang J. F. and Yang L. M., Chin.Chem Lett **2003,** 14, 1093
12. Mandal G,Bhattacharya S, Das S,Ganguly T,J Nanosci Nanotechnol. **2012,** 12, 187

13. Chakraborty A, Chakraborty S, Ganguly T Ind J Phys**2013**, *87,* 1113
14. Bhattacharya S, Mandal G, Chowdhury J, Ganguly T, Chem Phys Letts **2009,** 478, 215.
15. Mitra I., Paul S., Bardhan M., Das S, Saha M, Saha A,Ganguly T. Chem Phys Letts **2019**, 726, 1.
16. Ganguly T., Sharma D.K., Gauthier S., Gravel D., Durocher G.,J. Phys. Chem. **1992,** 96, 3757.
17. Rehm D., Weller A., Ber. Bunsen-Ges. Phys. Chem. **1969,** 73, 834.
18. Choi W,Lahiri I, Seelaboyina R, KangY S Critical Reviews in Solid State and Materials Sciences, **2010,** 35, 52.

INDIAN JOURNAL OF THEORETICAL PHYSICS, VOL 67, NOS. 1 & 2, 2019

Equilibrium Positions of a Cable-connected Satellites System in the Neighbourhood of Main Resonance

Sangam Kumar

P. G. Department of Physics,

L. S. College, B. R. A. Bihar University,

Muzaffarpur- 842001, Bihar, India

Mobile No.: +91-9905222295

E-mail: kumarsangam.phy@gmail.com

[Abstract: The equilibrium positions of non-linear planar oscillation of motion of a system of two cable-connected artificial satellites under the influence of earth's magnetic field, solar radiation pressure, shadow of the earth and earth's oblateness in the neighbourhood of the main resonance is studied. B. K. M. method is applied to study the resonant oscillation of the system. Eccentricity of elliptic orbit of the centre of mass of the system is considered as a small parameter. Here, no equilibrium position of motion of the system is found to exist in the neighbourhood of the main resonance.]

Key words: Cable-connected satellites, Elliptic orbit, Equilibrium position, B. K. M. Method, Main resonance.

1. Introduction

The present work is an attempt towards the generalization of work done by Bogoliubov[1], Beletsky and Novikova[2] and Beletsky[3]. They studied the motion of a system of two satellites connected by a light, flexible and inextensible string in the central gravitational field of force relative to its centre of mass. This study assumed that the two satellites are moving in the plane of the centre of mass of the system. Singh and Demin[8] and Singh[9] investigated the problem in two and three dimensional cases. Das et al.[4] studied the effect of magnetic force on the motion of a system of two cable-connected satellites in orbit. Kumar and Bhattacharya[5] studied the stability of equilibrium positions of two cable-connected satellites under the influence of solar radiation pressure, earth's oblateness and earth's magnetic field.

Equilibrium positions of the motion of a system of two cable-connected artificial satellites under the influence of solar radiation pressure, earth's oblateness, shadow of the earth and earth's magnetic field in the neighbourhood of main resonance is discussed. In fact, resonance can occur in both linear and non-linear system. The paper is concerned with non-linear system. The case of elliptical orbit of the centre of mass of the system is discussed. Shadow of the earth is taken to be cylindrical and the system is allowed to pass through the shadow beam. The satellites are connected by a light, flexible, inextensible and non-conducting cable. The satellites are taken as charged material particles. Charges are assumed to be small so that interaction between them may be neglected. Since masses of the satellites are small and distances between the satellites and other celestial bodies are very large, the gravitational forces of attraction between the

satellites and other celestial bodies including the sun have been neglected.

1. Equation of motion of the system

We write equations of motion of one of the satellites when the centre of mass moves along Keplarian elliptical orbit in Nechvile's co-ordinate system[6] as Prasad & Kumar[7]

$$X'' - 2Y' - 3X\rho = \lambda_a X - \frac{A}{\rho}\cos i - \gamma\left(\frac{B_1}{m_1} - \frac{B_2}{m_2}\right)\cos\epsilon\cos(v-\alpha) + \frac{12\mu K_2}{R^5}\rho X\left(\frac{m_1+m_2}{m_1}\right)$$

and

$$Y'' + 2X' = \lambda_a Y - \frac{A\rho'}{\rho^2}\cos i + \gamma\left(\frac{B_1}{m_1} - \frac{B_2}{m_2}\right)\cos\epsilon\sin(v-\alpha) - \frac{3\mu k_2}{R^5}\rho Y\left(\frac{m_1+m_2}{m_1}\right) \quad \ldots(1)$$

Condition of constraint is

$$X^2 + Y^2 \leq \frac{1}{\rho^2} \quad \ldots (2)$$

Also, $\rho = \dfrac{1}{(1+e\cos v)}$

$$A = \left(\frac{m_1}{m_1+m_2}\right)\left(\frac{Q_1}{m_1} - \frac{Q_2}{m_2}\right)\frac{\mu_E}{\sqrt{\mu p}},$$

$$K_2 = \frac{\bar{\varepsilon}\,\mathrm{Re}^2}{3}, \bar{\varepsilon} = \alpha_R - \frac{m}{2}, m = \frac{\Omega^2\,\mathrm{Re}}{g_e}$$

and

$$\lambda_a = \frac{p^3\rho^4}{\mu}\left(\frac{m_1+m_2}{m_1 m_2}\right)\lambda \quad \ldots (3)$$

m_1 and m_2 are masses of the two satellites. μ is the product of mass of the earth and gravitational constant. i is inclination of the orbit with the

equatorial plane, v is the true anomaly of the centre of mass of the system. B_1 and B_2 are the absolute values of the forces due to the direct solar pressure exerted on m_1 and m_2 respectively and are small. ε is inclination of the oscillatory plane of the masses m_1 and m_2 with the orbital plane of the centre of mass of the system. α is inclination of the ray. R is the position vector of the centre of mass of the system. e is the eccentricity of the orbit. Q_1 and Q_2 are charges of the two satellites. μ_E is the value of magnetic moment of the earth's di-pole. p is the focal parameter. Ω is angular velocity of the earth's rotation. g_e is the force of gravity. *Re* is equatorial radius of the earth. α_R is the earth's oblateness. λ is undetermined Lagrangian multiplier arising due to constraint for the finite length of the cable. γ is a shadow function. If γ is equal to zero, then the system is affected by the shadow of the earth. If γ is equal to one, then the system is not within the said shadow. Prime denotes differentiation with respect to *v*.

If motion of one of the satellites m_1 be determined with the help of equation (1), motion of the other satellite of mass m_2 can be determined by Prasad & Kumar[7]

$$m_1\bar{\rho}_1 + m_2\bar{\rho}_2 = 0 \qquad \ldots(4)$$

Where $\bar{\rho}_1$ and $\bar{\rho}_2$ are position vectors in the centre of mass system.

We transform the above two equations of (1) to the polar form by

$$X = (1 + e\cos v)\cos\Psi$$

$$\text{and} \quad Y = (1 + e\cos v)\sin\Psi \qquad \ldots(5)$$

Ψ is the angle between X-axis and the radius vector $(1+ e\cos v)$.

Substituting the derivatives obtained from expression (5) in equations (1), multiplying the first equation so obtained by $\sin\Psi$ and the second by $\cos\Psi$ and then subtracting the first from the second we obtain,

$$(1+e\cos v)\Psi'' - 2e\Psi'\sin v - 2e\sin v + 3\sin\Psi\cos\Psi$$
$$= A\ \cos i\ [(1+e\cos v)\sin\Psi - e\sin v\cos\Psi\ ] + \gamma\left(\frac{B_1}{m_1} - \frac{B_2}{m_2}\right)$$
$$.\cos\varepsilon\sin(\Psi + v - \alpha) - \frac{15\mu K_2}{R^5}\left(\frac{m_1+m_2}{m_1}\right)\sin\Psi\cos\Psi \qquad \ldots(6)$$

Since A is a small quantity, we write $A = eA_1$. Next we put $2\psi = \delta$, $3 = n^2$

$$\left(\frac{B_1}{m_1} - \frac{B_2}{m_2}\right)\cos\epsilon = eC \text{ and } \frac{15\mu k_2}{R^5}\left(\frac{m_1+m_2}{m_1}\right) = eD \qquad \ldots(7)$$

in equation of motion (6), retain terms up to the first order of small quantities and obtain

$$\delta'' + n^2\delta = e[\bar{\alpha}(\delta - \sin\delta) + 4\sin v - \delta''\cos v + 2\delta'\sin v + 2A_1$$
$$.\cos i\sin\delta/2 + 2C\gamma\sin\{\delta/2 + (v-\alpha)\} - D\sin\delta] \qquad \ldots(8)$$

with

$$f_o(a,\theta,v) = \bar{\alpha}(\delta - \sin\delta) + 4\sin v - \delta''\cos v + 2\delta'\sin v + 2A_1$$
$$.\cos i\sin\delta/2 + 2C\gamma\sin\{\delta/2 + (v-\alpha)\} - D\sin\delta \qquad \ldots(9)$$

Equation (8) may be interpreted as the equation of oscillation of a mechanical system having unit mass and a natural frequency n, under some non-linear perturbations explicitly depending on time.

2. Solution to the equation of motion of the system

According to Bogoliubov et. al.[1] method, solution in the 1st approximation of equation (8) at the main resonance $n = 1$ will be assumed to be of the form

$\delta = a\cos\phi\ ;\ \phi = v + k$ …(10)

where amplitude a and phase k satisfy the following equations

$\frac{da}{dv} = e\overline{A}_1(a,k)$ and $\frac{dk}{dv} = (n-1) + e\overline{B}_1(a,k)$ …(11)

$\overline{A}_1$ and $\overline{B}_1$ are the particular solution periodic with respect to k of the following system of partial differential equations

$$(n-1)\frac{\partial\overline{A}_1}{\partial k} - 2an\overline{B}_1 = \frac{1}{2\pi^2}\sum_{\sigma=\infty}^{-\infty} e^{j\sigma\theta}\int_0^{2\pi}\int_0^{2\pi} f_0\,(a,v,\phi)$$

$$.\,e^{-j\sigma\theta'}\cos\phi\,dv\,d\phi$$

$$a(n-1)\frac{\partial\overline{B}_1}{\partial k} + 2n\overline{A}_1 = -\frac{1}{2\pi^2}\sum_{\sigma=\infty}^{-\infty} e^{j\sigma\theta}\int_0^{2\pi}\int_0^{2\pi} f_0\,(a,v,\phi)$$

$$.\,e^{-j\sigma\theta'}\sin\phi\,dv\,d\phi$$

$\theta = \phi - v = \theta' = k, j = \sqrt{-1}$ …(12)

Further, it is known that

$$\sin(a\cos\phi) = 2\sum_{m=0}^{\infty}(-1)^m J_{2m+1}(a)\cos(2m+1)\phi$$

and

$$\cos(a\cos\phi) = J_0(a) + 2\sum_{m=1}^{\infty}(-1)^m J_{2m}(a)\cos 2m\,\phi \quad \ldots(13)$$

$J_0(a), J_{2m}(a), J_{2m+1}(a)$ are Bessel's functions of order 0, $2m$, $2m+1$ respectively.

With the help of (10),(11) and (13), (9) can be written as

$$f_0(a,v,\phi) = \bar{\alpha}\left[a\cos\phi - 2\sum_{m=0}^{\infty}(-1)^m J_{2m+1}(a)\cos(2m+1)\phi\right]$$

$$+4\sin v - \cos v\left[\left\{e\frac{d\overline{A}_1}{dv} - 2ane\overline{B}_1 - an^2\right\}\cos\phi\right.$$

$$-\left\{2ne\overline{A}_1 + ae\frac{d\overline{B}_1}{dv}\right\}\sin\phi] + 2\sin v[e\overline{A}_1\cos\phi - a(n + e\overline{B}_1)\sin\phi]$$

$$+ 4A_1\cos i\sum_{m=0}^{\infty}(-1)^m J_{2m+1}\left(\frac{1}{2}a\right)\cos(2m+1)\phi$$

$$+2C\gamma[2\sum_{m=0}^{\infty}(-1)^m J_{2m+1}\left(\frac{1}{2}a\right)\cos(2m+1)\phi\cos(v-\alpha)$$

$$+J_0\left(\frac{1}{2}a\right)\sin(v-\alpha) + 2\sum_{m=1}^{\infty}(-1)^m J_{2m}\left(\frac{1}{2}a\right)\cos 2m\phi\sin(v-\alpha)]$$

$$-2D\sum_{m=0}^{\infty}(-1)^m J_{2m+1}(a)\cos(2m+1)\phi \qquad \ldots(14)$$

Using (14) in (12), we get

$$(n-1)\frac{\partial\overline{A}_1}{\partial k} - 2an\overline{B}_1 = \frac{n^2}{e}[a - 2J_1(a)] - 4\sin k + 4A_1\cos i\,J_1\left(\frac{1}{2}a\right)$$

$$-2C\gamma J_0\left(\frac{1}{2}a\right)\sin(k+\alpha) + C\gamma J_2\left(\frac{1}{2}a\right)\frac{e^{j(k+\alpha)}}{j} - 2DJ_1(a)$$

and

$$a(n-1)\frac{\partial\overline{B}_1}{\partial k} + 2n\overline{A}_1 = -4\cos k - 2C\gamma J_0\left(\frac{1}{2}a\right)\cos(k+\alpha)$$

$$- C\gamma J_2(\tfrac{1}{2}a)e^{j(k+\alpha)} \qquad \ldots(15)$$

These are coupled partial differential equations giving

$$\overline{A}_1 = -\left[\frac{4\cos k}{(n+1)} + \frac{2C\gamma J_0\left(\frac{1}{2}a\right)\cos(k+\alpha)}{(n+1)}\right.$$

$$\left. + \frac{C\gamma J_2\left(\frac{1}{2}a\right)e^{j(k+\alpha)}}{(3n-1)}\right] \qquad \ldots(16)$$

and

$$\overline{B}_1 = \frac{(n-1)}{2an}\left[\frac{4\sin k}{(n+1)} + \frac{2C\gamma J_0\left(\frac{1}{2}a\right)\sin(k+\alpha)}{(n+1)} - \frac{jC\gamma J_2\left(\frac{1}{2}a\right)e^{j(k+\alpha)}}{(3n-1)}\right]$$

$$-\frac{1}{2}an\left[\frac{n^2}{e}[a - 2J_1(a)]\right.$$

$$+ 4\sin k - 4A_1\cos i J_1\left(\frac{1}{2}a\right) + 2C\gamma J_0\left(\frac{1}{2}a\right)\sin(k+\alpha)$$

$$\left. + jC\gamma J_2\left(\frac{1}{2}a\right)e^{j(k+\alpha)} + 2DJ_1(a)\right] \quad \ldots(17)$$

3. Equilibrium positions of the system

In order to obtain equilibrium positions of the system, we must have $\frac{da}{dv} = 0$ and $\frac{dk}{dv} = 0$ …(18)

Next, from (11), (16) and (17), we get after retaining powers of "a" upto fourth order in the Bessel's functions and with the suitable values $e = 0.01, \alpha = 30°, C = 0.1, \gamma = 0.5$ and $n = 1.2$

$$-6.373 \times 10^{-7}\cos(k+30°)a^4 + 2.24 \times 10^{-5}\cos(k+30°)a^2$$
$$-9.090 \times 10^{-4}\cos(k+30°) - 0.018\cos k = 0 \quad \ldots(19)$$

Again with the suitable values $A = 0.001, i = 0°, D = 0.2$, we obtain likewise

$$11.374 \times 10^{-7}\sin(k+30°)a^4 - 0.0375455a^3 - 3.4358 \times 10^{-5}$$
$$.\sin(k+30°)a^2 + 0.1002085a + 18.178 \times 10^{-3}\sin k + 0.9079 \times$$
$$10^{-3}.\sin(k+30°) = 0 \quad \ldots(20)$$

Clearly, equations (19) and (20) have been obtained for the value of frequency greater than unity. For frequency less than unity, roots of these equations are complex and therefore non-observable.

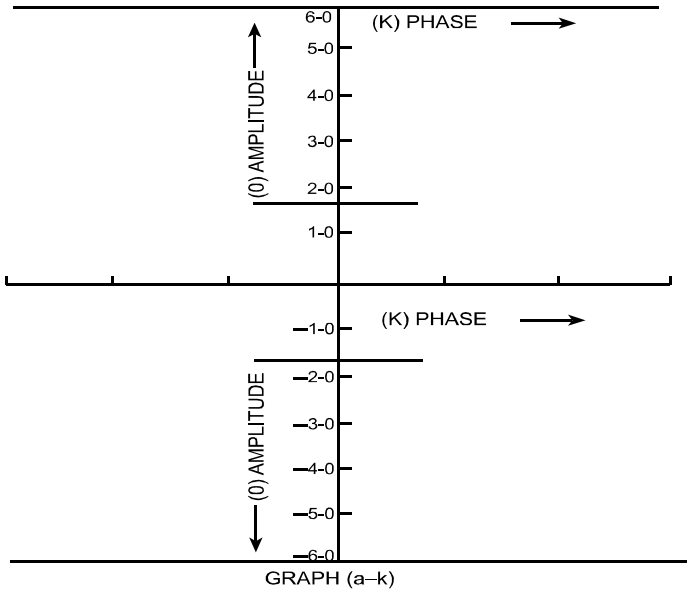

The algebraic solution of (19) and (20) is difficult. Hence, the equations are solved by graphical method as shown in the figure above.

4. *Conclusion*

We see from the graph that they do not intersect anywhere. Therefore, no equilibrium position of motion of the system exists.

Acknowledgement

I am thankful to Prof. R. K. Sharma, former Scientist from VSSC Trivandrum for his encouragement and support.

References

1. Bogoliubov N.N., Krylov and Mitropolsky, Y.A.- Asymptotic Methods in Theory of Non-linear Oscillation, Hindustan Pub. Corp., Delhi, pp. 201-208 (1961).

2. Beletsky V.V. and Novikova E.T.- Kosmicheskie Issledovania, **7(6)**, pp. 377-384 (1969).
3. Beletsky, V.V.- Kosmicheskie Issledovania, **7(6)**,pp. 827-840 (1969).
4. Das S.K., Bhattacharya P.K. and Singh R.B.- Proc. Nat. Acad. Sci. India, **46(A)**, pp. 287-299 (1976).
5. Kumar S. and Bhattacharya P.K.- Proc. Workshop on Sp. Dyn. & Celes. Mech., Muz., India, Eds. K. B. Bhatnagar & B. Ishwar, pp. 71-74 (1995).
6. Nechvile V.- Acad. Paris Compt. Rend., **182**, pp. 310-322 (1926).
7. Prasad J.D. and Kumar S.- Jour. Purv. Acad. Sci. Jaunpur, India, **17** (Phy.Sci.), pp. 27-34 (2011).
8. Singh R.B. and Demin, V.G.- Celestial Mechanics, **6**, pp. 268-277 (1972).
9. Singh R.B.- Astronautica Acta, **18**, pp. 301-308 (1973).

———————

INDIAN JOURNAL OF THEORETICAL PHYSICS, VOL 67, NOS. 1 & 2, 2019

On Goldstein's Approximation of Energy Transfer Spectrum to a Two-phase Homogeneous Turbulent Flow.

S. K. SAHA

M. C. Centre for mathematics and mathematical sciences,

Kolkata – 700025.

Residential address: 18/348, Kumar Lane, Chinsurah, Hooghly,

Pin – 712101, West Bengal, India.

Email: sksaha30@gmail.com

H. P. Mazumdar,

Honorary visiting professor, PAMU, Indian Statistical Institute,

Kolkata – 700108.

Email: hpmi2003@yahoo.com

[Abstract: In this paper we have applied the Goldstein's approximation and determine the energy spectrum and the behaviours at small wave numbers $(k \to 0)$ and for large wave numbers $(k \to \infty)$. For these cases , we have dealt with the asymptotic behaviours of the energy spectrum through Sen's approach of self-preserving theory of homogeneous turbulence. In the present analysis we learned ourselves to the cases where various dissipation is not important. In these process we have discussed several power laws and their importance at small wave numbers . They are analysed with appropriate criticism.]

1. Introduction

In this paper , we deal herewith the general approximation of Goldstein to a particle- ladden two phase homogeneous isotropic turbulent flow. In recent times much attention is paid to the prediction of particle-ladden turbulent flows as they occur in many technologically important areas. Research interest in these flows are generally two –fold e.g., Islam and Mazumdar [1] considered the effect of turbulence on the particle concentration field and the modification of turbulence by the particles. We shall be concerned here with certain aspect of the problem how turbulence is modified by the particles when they are present in the flow in large enough concentration (Squares and Eaton[2]).

Theoretical investigations were carried out in this area by Tchen[3], Meck and Jones[4], Reeks[5], Nir and Pismen[6] and others. Most of these works involve studies of the influence of particle inertia on the turbulent dispersion process. General confirmations of the conclusions made in these studies, were obtained from the experiments (Wells and Stock[7], Snyder and Lumley[8]). Reeks[9], Elghobashi and Truesdell[10], Yeung and Pope[11] and Squares and Eaton[2] have carried out numerical simulation of particle-ladden turbulent flows. It is difficult to make proper interpretations of the experimental data as they are valid only for the conditions of the experiment and can not be generalized (Elghobashi and Truesdell[12]). For example, when fine droplets (or particles) of diameters $\leq 250\mu$ are injected in a free turbulent jet, the turbulent intensity decreases, lowering the spreading rate of the half width of the jet, whereas the

addition of the large particles of diameters $\geq 500\mu$ causes an increase in the turbulent intensity. Hardalupas et al[13] observed opposite phenomena in their experimental investigation on a particle-ladden turbulent flow.

Rao[14] studied the final period decay of energy spectrum of a particle-ladden homogeneous isotropic turbulence by a similarity process. In the present paper an attempt is made to examine the similarity features of the decay of turbulence kinetic energy spectrum in a particle-ladden homogeneous isotropic turbulent flow. We shall assume that the size of the particles is sufficiently large so that the turbulence is attenuated by the dispersed phase.

2. Formulation of the problem

The spectral equation governing the decay of turbulence kinetic energy in a particle-ladden homogeneous isotropic turbulent flow, is given by (Baw and Peskin[15], Tsuji[16])

$$\frac{\partial}{\partial t} E(k,t) = T(k,t) - 2\nu k^2 E(k,t) - 2\beta \frac{\nu k^2}{\frac{1}{\tau} + \nu k^2} E(k,t), \ldots (2.1)$$

where k is the wave number, ν is the kinematic viscosity, τ is the characteristic time $= \frac{2}{9}\frac{\rho_s \sigma^2}{\mu}$, $\rho_s$is the density of the solid material , σ is the radius of the particle, μ is the co-efficient of viscosity, $\beta = \frac{\rho_p}{\rho\tau}$, ρ_p is the volume concentration of the solid phase in the flow, ρ is the density of the gas,

$E(k, t) = 2\pi k^2 \varphi_{ii}(k, t)$, $\varphi_{ij}(k, t)$ ... (2.2)

being the Fourier transform of $\overline{v_i v'_j}$, the correlation between the fluctuating gas velocity components v_i and v'_j pertaining to the points $P(\vec{X})$ and $P'(\vec{X})$ inside the flow field;

$T(k,\ t)\ =\ 2\pi k^2\Gamma_{ii}(k,\ t)$, $\Gamma_{ij}(k,\ t)$ is the Fourier transform of $\frac{\partial}{\partial r_k}(\overline{v_i v_k v_j'}\ -\ \overline{v_i v_j' v_k'}),\vec{r}\ =\ \overline{X'}\ -\ \vec{X}.)$ ...(2.3)

The term on the left hand side of (2.1), describes the rate at which turbulence kinetic energy changes. The first term on the right hand side of (2.1) represents the transfer of kinetic energy at the wave number k due to turbulence self interactions. The second term describes the dissipation of turbulence kinetic energy due to the effects of molecular viscosity. The third term takes account of the effect due to the presence of particles, which are so massive that they are unaffected by the gas turbulent fluctuations (Wallace[17]). In the next section we seek self-preserving solution of equation (2.1).

3. Application of Goldstein's approximation for the energy transfer spectrum function to two-phase homogeneous turbulent flow: Self-preserving solution for the turbulence energy spectrum

In order to solve equation (2.1), the energy transfer spectrum T(k, t) is to be modeled. We accept the local form for T(k, t), as suggested by S. Goldstein[18], e.g.,

$$T(k,t)\ =\ -2\gamma_2\frac{d}{dk}\left\{\int_k^\infty [E(k_1,t)]^n k_1^m\, dk_1\right\}^c$$

$$\left\{\int_0^k [E(k_2\ ,t)]^{n_1}\, k_2^{m_1}\, dk_2\right\}^{c_1} \qquad \ldots(3.1)$$

which satisfies only dimensional requirements

$$nc\ +\ n_1c_1\ =\ \frac{3}{2},(m\ +1)c\ +\ (m_1+\ 1)c_1\ =\ \frac{5}{2}, \qquad \ldots(3.2)$$

where γ_2 is a non-dimensional constant.

Substituting (3.1) in (2.1) we obtain

$$\frac{\partial}{\partial t}E(k,t)$$

$$= -2\gamma_2 \frac{d}{dk}\left\{\int_k^\infty [E(k_1,t)]^n k_1^m \, dk_1\right\}^c \left\{\int_0^k [E(k_2,t)]^{n_1} k_2^{m_1} \, dk_2\right\}^{c_1}$$

$$- 2\nu k^2 E(k,t) - 2\beta \frac{\nu k^2}{\frac{1}{\tau} + \nu k^2} E(k,t). \qquad \ldots (3.3)$$

Based on the assumption that particles are essentially unaffected by the turbulence fluctuations, we may set

$$\frac{1}{\tau} \ll k^2 \qquad \ldots (3.4)$$

It is to be remarked that when the condition (3.4) is satisfied, for every high frequency fluctuations of gas, gas-solid velocity correlations are negligible as the response time of the particle is sufficiently long (Wallace[17]).

In view of the relation (3.4), the equation (3.3) is reducible to

$$\frac{\partial}{\partial t}E(k,t)$$

$$= -2\gamma_2 \frac{d}{dk}\left\{\int_k^\infty [E(k_1,t)]^n k_1^m \, dk_1\right\}^c \left\{\int_0^k [E(k_2,t)]^{n_1} k_2^{m_1} \, dk_2\right\}^{c_1}$$

$$- 2\nu k^2 E(k,t) - 2\beta E(k,t). \qquad \ldots (3.5)$$

We seek a general type of self-preserving solution of (3.5) in the form (Sen[19])

$$E(k,t) = \frac{1}{\alpha^2 k_0^3 t_0^2} \frac{s^3}{\tau^2} f\left(\frac{sk}{k_0}\right), \qquad \ldots (3.6)$$

where α, k_0 , t_0 are constants, $\tau = \frac{t}{t_0}$.

Substituting (3.6) in (3.5) we obtain after simplifications

$$(3c - 2)f(x) + cxf'(x) + 2MA\sqrt{R}f(x)$$
$$= -\frac{2\gamma_2}{\alpha}\frac{d}{dx}\left[\left\{\int_x^\infty [f(x_1)]^n x_1^m\, dx_1\right\}^c \left\{\int_0^x [f(x_2)]^{n_1} x_2^{m_1} dx_2\right\}^{c_1}\right]$$
$$-\frac{2\nu}{Re}\frac{\tau}{s^2}x^2 f(x), \qquad \ldots (3.7)$$

where

$$x = \frac{sk}{k_0}, \text{Re} = \text{Reynolds number} = \frac{1}{\nu k_0^2 t_0}, c = \frac{\tau s_\tau}{s}, s_\tau = \frac{\partial s}{\partial \tau}.$$

$$R = \frac{\varepsilon t^2}{\nu}, M = \frac{\rho_p}{\rho} = (\frac{\rho_p}{\tau\rho}).\tau = \beta\tau, A = \frac{1}{\tau}\sqrt{\frac{\nu}{\varepsilon}}.$$

When the turbulence is characterized by very large Reynolds numbers $Re \to \infty$, the equation (3.7) is reduced to

$$(3c - 2)f(x) + cxf'(x) + 2MA\sqrt{R}f(x) + \frac{2\gamma_2}{\alpha}\frac{d}{dx}$$
$$\left[\left\{\int_x^\infty [f(x_1)]^n x_1^m\, dx_1\right\}^c \left\{\int_0^x [f(x_2)]^{n_1} x_2^{m_1} dx_2\right\}^{c_1}\right] = 0. \qquad \ldots (3.8)$$

Clearly equation (3.8) may admit self-preserving solution for different choices of MA if $R = \frac{\varepsilon t^2}{\nu}$ remains constant during decay process. Usually, R = constant applies to the wave number range of the energy containing eddies and it need not apply to equilibrium range of wave number. In order to describe the self-preserving features of the turbulence energy spectrum, Heisenberg[20] assumed that the energy containing eddies would be in quasi- equilibrium, so that we may consider them as if they are in equilibrium as far as possible in view of their finite rate of decay (Hinze[21]). We accept this

premise for our analysis of the present case. Let us discuss asymptotic behaviour of *f(x)* for the cases (i) $x \to 0$ and (ii) $x \to \infty$, when turbulence is characterized by very large Reynolds number $Re \to \infty$.

Case I: Let

$f(x) \sim Bx^p \; as \; x \to 0$; B is a non-zero constant and $p > 0$. ... (3.9)

Substituting (3.9) in equation (3.8), we obtain, after some calculation,

$$\left[(3c - 2) + pc + 2MA\sqrt{R}\right]x^p - \frac{\gamma_2\sqrt{B}}{\alpha(m + np + 1)^c(m_1 + pn_1 + 1)^{c_1}}(3p + 5)x^{\frac{3p+3}{2}} = 0. \quad \ldots (3.10)$$

Now if $p < \frac{3p+3}{2}$, then the first term of the equation (3.10) is significant. Equating the coefficient of x^p to zero, we obtain

$$p = \frac{2-3c}{c} - \frac{2MA\sqrt{R}}{c}, for \; MA\sqrt{R} < \frac{2-3c}{2}. \quad \ldots (3.11)$$

The family of solutions given in (3.11) have the asymptotic behaviour

$$f(x) \sim x^{\frac{2-3c}{c} - \frac{2MA\sqrt{R}}{c}}, (x \to 0), for \; MA\sqrt{R} < \frac{2-3c}{2}. \quad \ldots (3.12)$$

For $c = \frac{1}{2}$, (3.11) yields

$$f(x) \sim x^{1-4MA\sqrt{R}}, (x \to 0), for \; MA\sqrt{R} < \frac{1}{4}, \quad \ldots (3.13)$$

which corresponds to the Heisenberg's type spectrum law

$$E(k,t) \sim k^{1-4MA\sqrt{R}}, (k \to 0), for \; MA\sqrt{R} < \frac{1}{4}. \quad \ldots (3.14)$$

Putting $c = \frac{2}{5}$, in (3.11) we obtain

$$f(x) \sim x^{2-5MA\sqrt{R}}, (x \to 0), for\ \ MA\sqrt{R} < \frac{2}{5}, \quad \ldots (3.15)$$

which corresponds to the spectrum law

$$E(k,t) \sim\ k^{2-5MA\sqrt{R}}, (k \to 0), for\ \ MA\sqrt{R} < \frac{2}{5}. \quad \ldots (3.16)$$

Again putting $c = \frac{1}{3}\ in$ (3.11) we obtain

$$f(x) \sim x^{3-6MA\sqrt{R}}, (x \to 0), for\ \ MA\sqrt{R} < \frac{1}{2}, \quad \ldots (3.17)$$

which corresponds to the spectrum law

$$E(k,t) \sim\ k^{3-6MA\sqrt{R}}, (k \to 0), for\ \ MA\sqrt{R} < \frac{1}{2}. \quad \ldots (3.18)$$

Further if we put $c = \frac{2}{7}$, in (3.11) we obtain

$$f(x) \sim x^{4-7MA\sqrt{R}}, (x \to 0), for\ \ MA\sqrt{R} < \frac{4}{7}, \quad \ldots (3.19)$$

which corresponds to the Loitsianky type spectrum law

$$E(k,t) \sim\ k^{4-7MA\sqrt{R}}, (k \to 0), for\ \ MA\sqrt{R} < \frac{4}{7}. \quad \ldots (3.20)$$

The constant of proportionality being Loitsiansky's constant if *MA* = 0 (cf. Loitsiansky[22], Lin[23] and Batcheler[24]).

Finally if we put $c = \frac{2}{9}$, in (3.11) we obtain

$$f(x) \sim x^{6-9MA\sqrt{R}}, (x \to 0), for\ \ MA\sqrt{R}\ < \frac{2}{3}, \quad \ldots (3.21)$$

which corresponds to the spectrum law

$$E(k,t) \sim\ k^{6-9MA\sqrt{R}}, (k \to 0), for\ \ MA\sqrt{R} < \frac{2}{3}. \quad \ldots (3.22)$$

In the case when *MA = 0*, then (3.22) reduces to

$E(k,t) \sim k^6 \ (k \rightarrow 0)$. ...(3.23)

In this case no transfer of energy takes place from mechanical motions to magnetic fields.

Case II: Let

$f(x) \sim B'x^{-p}$ as $x \rightarrow \infty$; B' is a non-zero constant and $p > 0$. ... (3.24)

Taking (3.24) into account, equation (3.8) is reducible to

$$\left[(3c-2) - pc + 2MA\sqrt{R}\right]x^{-p} - \frac{\gamma_{2B'\sqrt{B'}}}{\alpha(m-np+1)^c(m_1 - pn_1 + 1)^{c_1}}(5 - 3p)x^{\frac{-3p+3}{2}} = 0. \quad \ldots (3.25)$$

It can be easily seen that the second term on the left hand side of (3.25) is predominant if $p<3$. Accepting this we equate the co-efficient of $x^{\frac{3(1-p)}{2}}$ to zero and obtain $p = \frac{5}{3}$. Thus in the case when the turbulence is characterised by sufficiently large Reynolds number the asymptotic behaviour of $f(x)$ as $x \rightarrow \infty$ is given by

$f(x) \sim x^{-\frac{5}{3}} \ (x \rightarrow \infty)$. ... (3.26)

This gives

$E(k,t) \sim k^{-\frac{5}{3}} \ (k \rightarrow \infty)$. ... (3.27)

In this case the energy spectrum behaves the well known Kolmogorov's spectrum - $\frac{5}{3}$.

4. Concluding remarks

In the last section we have discussed some asymptotic similarity solutions of importance for values of $k \to 0$ and $k \to \infty$ with $0 < c < \frac{2}{3}$. Parametric values of c being chosen to be $c = \frac{1}{2}, c = \frac{2}{5}, c = \frac{1}{3}$ and $c = \frac{2}{7}$. An additional case may be chosen as $c = \frac{2}{9}$ $(c < \frac{2}{3})$ being found to hold for similarity solution at small and large wave numbers. The results clearly show that the self-preserving solutions are admitted for different values of $MA(M = \frac{\rho_p}{\rho}, A = \frac{1}{\tau}\sqrt{\frac{\nu}{\varepsilon}})$ and $R(= \frac{\varepsilon t^2}{\nu})$ during the process of decay. When $MA = 0$, this case may be compared to the situation when no transfer of energy takes place from mechanical motion to the magnetic field (Chandrashekhar[1]). For this case energy spectrum $E(k,t) \sim k^6$ $(k \to 0)$.

Surprisingly it is observable that several power laws exhibited by the energy spectra for different values of $MA\sqrt{R}$ which are in turn dependent on the choice of the parameter c and finally all the energy spectra behaving so differently for small values of $k \to 0$ ultimately merge to the energy spectrum $E(k,t) \sim k^{-\frac{5}{3}}$; $(k \to \infty)$.

References

1. Islam N**.** and Mazumdar H. P.: Ind. J. Theo. Phys. **44** No. 1, 9-16 (1996),.
2. Squires K. D. and Eaton J. K.: Phys. Fluids, **42,** 1191 (1990).

3. Tchen C. M.: Ph. D. Dissertation , Delt, The Hague, Martinus Nijhoff (1947).

4. Meek C. C. and Jones B. G.: Atmos J. Sci. , **30**, 239 (1973).

5. Reeks M. W.: Mech. J. Fluid, **83**, 529 (1977).

6. Nir A. and Pisman L. M.: Mech. J. Fluid, **94**, 369 (1979).

7. Wells M. R. and Stock D. E.: Mech. J. Fluid, **136**, 31 (1983).

8. Snyder W. H. and Lumbey J. l.: Mech. J. Fluid**, 48,** 41 (1971).

9. Reeks M. W.: Mech. J. Fluid**, 97**, 569 (1980).

10. Elghobashi S. E. and Truesdell G. C.: Fluids, Phys. **A5,** 7th Symposium on turbulent shear flows, Stanford University (1989).

11. Yeung P. K. and Pope S. B.: Mech. J. Fluid, **207,** 531 (1989).

12. Elghobashi S. E. and Truesdell G. C.: Fluids, Phys. **A5,** 1790 (1993).

13. Hardalupus Y, Roy. et al , Proc. Soc. London, Sec **A 426**, 31 (1969).

14. Rao C. S.: Studies in two phase gas-s0lids flow, Ph. D. Dissertation, University of Houston, Houston , U. S. A. (1970).

15. Baw P. S. H. and Peskin R. L.: Technical Report No. 188- MAE, NYO2930-31, Department of Mechanical and Aerospace Engineering, Rutgers – The state University, New Brunswick, New Jersey (1968).

16. Tsuji Y.: In Encyclopedia of fluid Mechanics, edited by Cheremisinoff N. P., **4**, 283 (1986).

17. Wallace J. P.: A study of the fluid turbulence energy spectrum in a gas-solid suspension, Ph. D. Thesis, Rutgers University (1966).

18. Goldstein S.: On the law of decay of homogeneous isotropic turbulence and the theories of the equilibrium and similarity spectra, Proc. Cambridge Phil. Soc., **47,** 554-574, (1951).

19. Sen N. R.: The modern theory of turbulence, Indian association for the cultivation of science, Calcutta, (1956).

20. Heisenberg W.: Zeit Phys., **124**, 628 (1948).

21. Hinze J. O.: Turbulence, Mc Graw-Hill, New York (1975).

22. Loitsiansky L. G.: Rep.centr.Aero.Hydrodyn. Ins.(Moscow), No. 440 (translated as tech. Memor. Nat. Adv. Comm. Aero., Wash, No.1079), (1939).

23. Lin C. G.: Proc. I. St. Symp. In Appl. Math. Amer. Soc., 81, (1949),.

24. Batcheler G. C.: Proc. Roy. Soc., **A195,** 1043, 513 (1949).

———————

INDIAN JOURNAL OF THEORETICAL PHYSICS, VOL 67, NOS. 1 & 2, 2019

An All-optical Integrated Pauli X, Y, Z Quantum Gates with Frequency Encoding Technique

Baishali Sarkar[1,*] and Sourangshu Mukhopadhyay[2]

[1]Department of Physics, M. U. C. Women's College, Burdwan, W. B., India

[2] Department of Physics, The University of Burdwan, Golapbag, Burdwan, W. B., India.

email: -baishali22@gmail.com.

[Abstract : Frequency encoding technique is a well-established process to get very high speed optical computing and processing. In quantum computing this frequency encoding may be highly useful. In this paper the authors propose an all-optical integrated Pauli X, Y and Z logic system. This system uses the frequency encoding mechanism. As the proposed system uses no optical switch for its implementation, so speed of operation is very high, i.e., far above THz speeds.]

Keywords: Pauli X, Y, Z quantum logic gates, Frequency encoding, Phase lead/lag, Reversibility.

1. Introduction

The three Pauli's quantum logic gates are important in quantum optical computing for their advantages. They can very easily be used in qubit logic system[1-8] Several logic gates are designed to facilitate

* Corresponding author

information processing and computing in optical domain[9-14]. The one qubit X-logic gate operation is represented by the matrix $\begin{pmatrix}0 & 1\\ 1 & 0\end{pmatrix}$ andused to implement quantum NOT operation whereas the quantum Y-logic gate has the following operational characteristics-

$$Y\begin{pmatrix}C_0\\ C_1\end{pmatrix} = \begin{pmatrix}0 & -i\\ i & 0\end{pmatrix}\begin{pmatrix}C_0\\ C_1\end{pmatrix} = \begin{pmatrix}-iC_1\\ iC_0\end{pmatrix}$$

On the other hand, the quantum Z-logic gate flips one component of qubit retaining the other unchanged. The matrix representation of Z logic is $\begin{pmatrix}1 & 0\\ 0 & -1\end{pmatrix}$. Again, frequency encoding technique is an established one, which can offer several advantages in optical computing and parallel processing. Different all-optical digital operations like logic operation, memory function, counters etc. are already developed by the use of frequency encoding technique[15-18]. Here in this paper the authors propose a new method of developing an integrated Pauli *X, Y, Z* quantum logic system using frequency encoding principle. The important point of this integrated Pauli *X, Y* and *Z* quantum gate is that the whole scheme uses no optical/ optoelectronic switch; hence speed of operation is far beyond *THz* limit.

2. Frequency encoding technique

Several encoding/decoding techniques are used in optical communication and data processing systems. These are intensity encoding, phase encoding, polarization encoding, frequency encoding etc. In general, in intensity encoding certain reference intensity level of an optical signal is used to encode the logic state ‘1’ or ‘0’. But during signal transmission and execution of logic operations, the reference level

may vary due to absorption/attenuation of the signal in the channel/medium. To avoid this bit-error problem frequency encoding technique is the most reliable and faithful encoding technique in optical communication. Here the frequencies (ν_1 and ν_2) of two particular monochromatic light signals are considered to indicate the logic state '1' and '0' respectively.

3. Frequency encoded Pauli X-gate

Frequency encoded Pauli *X*-gate can be implemented in a very simple way. Two monochromatic light signals of frequencies ν_1 and ν_2 are considered as logical inputs 1 and 0 respectively and they are passed through a coupling device which only inverses the two input signals at the output. If ν_1 and $\nu_2$frequencies are taken as the inputs A and B(fig.1), the output will be received as $Y_1 = \nu_2$ and $Y_2 = \nu_1$ respectively. The whole process can be represented as

$X\begin{pmatrix}\nu_1\\ \nu_2\end{pmatrix} = \begin{pmatrix}0 & 1\\ 1 & 0\end{pmatrix}\begin{pmatrix}\nu_1\\ \nu_2\end{pmatrix} = \begin{pmatrix}\nu_2\\ \nu_1\end{pmatrix}$, which is Pauli's *X*-gate.

Fig.1 shows the block diagram of Pauli *X*-gate with an optical fiber based cross-coupling system. In the same way $\begin{pmatrix}\nu_2\\ \nu_1\end{pmatrix}$ will be converted to$\begin{pmatrix}\nu_1\\ \nu_2\end{pmatrix}$.

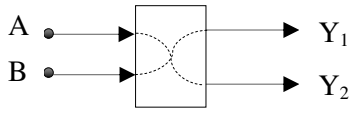

Coupling Device

Fig.1

Implementation of *Pa*uli X-gate with optical fiber based cross- coupling mechanism.

To test the reversibility, if the outputs are again given to inputs as $A = \nu_2$ and $B = \nu_1$, after passing through the coupling box, the initial input condition ($Y_1 = \nu_1$ and $Y_2 = \nu_2$) will be received at the output that is, $X\begin{pmatrix}\nu_2\\ \nu_1\end{pmatrix} = \begin{pmatrix}1 & 0\\ 0 & 1\end{pmatrix}\begin{pmatrix}\nu_2\\ \nu_1\end{pmatrix} = \begin{pmatrix}\nu_1\\ \nu_2\end{pmatrix}$. The truth table is shown in table 1.

Table 1

Inputs		Outputs	
A	B	Y_1	Y_2
ν_1 (0)	ν_2 (1)	ν_2 (1)	ν_1 (0)
ν_2 (1)	ν_1 (0)	ν_1 (0)	ν_2 (1)

Truth table of Pauli X-gate using frequency encoding mechanism.

4. Frequency encoded Pauli Y-gate

Fig.2 depicts the construction method of Pauli *Y*-gate. Here $\frac{\pi}{2}$ phase delay is introduced in one output arm of the proposed Pauli *X*-gate and $\frac{\pi}{2}$ phase lead is used in the other arm of the *X*-output simultaneously. The light signals of frequencies ν_1 and ν_2 are given as inputs to the terminals *A* and *B* respectively. After passing through the coupler where the frequencies are interchanged the first output signal of frequency ν_2 is sent through the $\frac{\pi}{2}$ phase delay. It develops the new output Y_1as $-i\nu_2$. The second part of the output having signal frequency ν_1 after suffering $\frac{\pi}{2}$ phase leading, the final output will be $i\nu_1$. So if the input signal representing $0(\nu_1)$ and $1(\nu_2)$ are represented by $E_A = E_0 e^{i(w_1 t + K_2 z)}$ and $E_B = E_0 e^{i(w_1 t + K_2 z)}$, then the outputs are $E_{Y_1} = E_0 e^{i(w_2 t + K_2 z - \pi/2)}$ and $E_{Y_2} = E_0 e^{i(w_1 t + K_1 z - \pi/2)}$. This process can be represented as $Y\begin{pmatrix}\nu_1\\ \nu_2\end{pmatrix} = \begin{pmatrix}0 & -i\\ i & 0\end{pmatrix}\begin{pmatrix}\nu_1\\ \nu_2\end{pmatrix} = \begin{pmatrix}-i\nu_2\\ i\nu_1\end{pmatrix}$.

If these two outputs are fed back to inputs the initial states will come back in the following way-

$$X\begin{pmatrix}-i\nu_2\\ i\nu_1\end{pmatrix} = \begin{pmatrix}0 & -i\\ i & 0\end{pmatrix}\begin{pmatrix}-i\nu_2\\ i\nu_1\end{pmatrix} = \begin{pmatrix}\nu_1\\ \nu_2\end{pmatrix}.$$

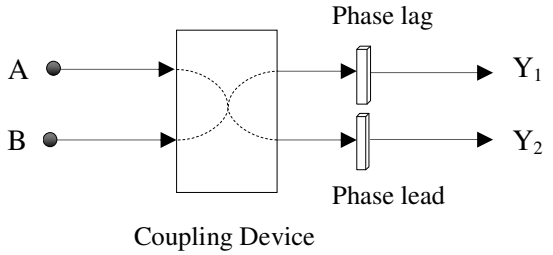

Fig.2

Implementation of Pauli *Y*-gate with fiber optic cross-coupling mechanism.

If the input states are represented by the optical fields $E_A = E_0 e^{i(w_2 t + K_2 z - \pi/2)}$ and $E_B = E_0 e^{i(w_1 t + K_1 z - \pi/2)}$ then the outputs will be $E_{Y_1} = E_0 e^{i(w_1 t + K_1 z)}$ and $E_{Y_2} = E_0 e^{i(w_2 t + K_2 z)}$. This process can be shown by a truth table

Table 2

Inputs		Outputs	
A	B	Y_1	Y_2
ν_1	ν_2	$-i\nu_2$	$i\nu_1$
$-i\nu_2$	$i\nu_1$	ν_1	ν_2

Truth table of frequency encoded Pauli *Y*-logic system.

5. Frequency encoded Pauli Z-gate

Quantum Pauli *Z*-logic gate reverses one component keeping the other one unchanged, so

$$Z\begin{pmatrix} C_0 \\ C_1 \end{pmatrix} = \begin{pmatrix} 1 & 0 \\ 0 & -1 \end{pmatrix}\begin{pmatrix} C_0 \\ C_1 \end{pmatrix} = \begin{pmatrix} C_0 \\ -C_1 \end{pmatrix}.$$

Using single phase leading component this gate can be implemented as shown in fig.3. Here two light signals of two different frequencies (ν_1 and ν_2) are considered as the inputs to the gate (A and B). The 1st input signal is carried directly to the output terminal $Y_1 = \nu_1$ while

the 2nd input signal ($B = \nu_2$) is sent through the phase leading system. This signal of frequency ν_2 suffers a $+\pi$ phase increment that is ν_2 frequency is treated as $-\nu_2$ after passing through the phase lead mechanism. Thus if the input signals are represented as $E_A = E_0 e^{i(w_1 t + K_1 z)}$ and $E_B = E_0 e^{i(w_2 t + K_2 z)}$, the outputs will be $E_{Y_1} = E_0 e^{i(w_1 t + K_1 z)}$ and $E_{Y_2} = E_0 e^{i(w_2 t + K_2 z)}$.

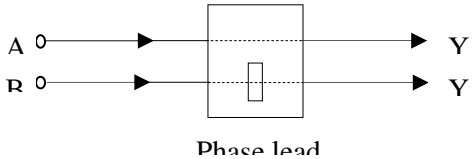

Fig. 3
Optical implementation of Pauli-*Z* logic gate.

When these outputs are again forwarded to the inputs A and B, the frequency $-\nu_2$ at B end will observe phase increment of $+\pi$ again which turns the $-\nu_2$ frequency to ν_2 frequency. So the outputs will be represented as $E_{Y_1} = E_0 e^{i(w_2 t + K_2 z)}$ and $E_{Y_2} = E_0 e^{i(w_2 t + K_2 z)}$, when the inputs will be $E_A = E_0 e^{i(w_1 t + K_1 z)}$ and $E_B = E_0 e^{i(w_2 t + K_2 z)}$.Hence the reversibility condition is fulfilled. The matrix representation of the scheme is shown below-

$$Z\begin{pmatrix}\nu_1\\ \nu_2\end{pmatrix}=\begin{pmatrix}1 & 0\\ 0 & -1\end{pmatrix}\begin{pmatrix}\nu_1\\ \nu_2\end{pmatrix}=\begin{pmatrix}\nu_1\\ -\nu_2\end{pmatrix} \text{ and}$$

$$Z\begin{pmatrix}\nu_1\\ -\nu_2\end{pmatrix}=\begin{pmatrix}1 & 0\\ 0 & -1\end{pmatrix}\begin{pmatrix}\nu_1\\ -\nu_2\end{pmatrix}=\begin{pmatrix}\nu_1\\ \nu_2\end{pmatrix}.$$ The truth table is given in table3.

Table 3

Inputs		Outputs	
A	B	Y_1	Y_2
ν_1 (0)	ν_2 (1)	ν_1 (1)	$-\nu_2$ (0)
ν_1 (1)	$-\nu_2$ (0)	ν_1 (0)	ν_2 (1)

Truth table of frequency encoded Pauli Z-logic gate.

6. Integrated quantum Pauli X, Y, Z gate

Shows an integrated scheme of Pauli *X, Y, Z* gate where three gates can operate simultaneously or individually. Here *A* and *B* are two common input terminals for the three quantum gates.

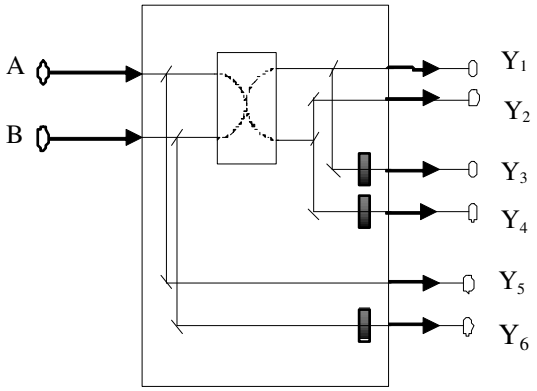

Fig.4

Optical scheme for implementing integrated Pauli *X,Y* and *Z* gates.

Y_1 and Y_2 are output terminals for *X*-gate, Y_3 and Y_4 are for *Y*-gate, Y_5 and Y_6 are the same for quantum Pauli *Z*-gate. If any two monochromatic optical signals of two different frequencies are given at the terminals *A* and *B* as inputs, then at the output ends the three quantum Pauli gates will be obtained in parallel. It is possible to access all the three gates at a time.

7. Conclusion

The whole scheme is all-optical and so it works with fastest operational speed. It is very interesting to note that no optical switch like SOA, EDFA etc. is used here. For this reason, it is highly cost effective. Again, the parallelism of optics is exploited here and so the integrated scheme of Pauli *X, Y* and *Z* gates are used very successfully.

References

1. Barz S. Fitzsimons, Kashefi J. F., E. and Walther, P. - Experimental verification of quantum computation, Nature Physics, 9, 727 (2013).
2. Álvarez A. M. Souza, Suter G. A. , D.- Robust dynamical decoupling for quantum computing and quantum memory, Phys. Rev. Lett.**106**,240501 (2011).
3. Yu, C. Yi, XX. Song H. Fan, H.-Entangling power in deterministic quantum computation with one qubit, Physical Review A, **87**, 022322 (2013).
4. Venkataraman, V. Saha, K. and Gaeta, A.L. -Phase modulation at the few-photon level for weak-nonlinearity-based quantum computing, Nature Photonics**, 7**,138 (2013).
5. Menicucci, Flammia N. C., S. T. Olivier - One-Way Quantum Computing in the Optical Frequency Comb., Phys Rev Lett**., 101**,13050 (2008).
6. Walmsley, I. - Linear Optical Quantum Computing in a Single Spatial Mode, American Physical Society, **59**, H4.1(2014).
7. Langford, Ramelow N. K., PrevedelS., Munro R., Milburn W. J., Zeilinger G. J., A. - Efficient quantum computing using coherent photon conversion, Nature, **478**, 360 (2011).
8. Liang, Beige Y., L. A. and Kwek, L. C. - Repeat-Until-Success Linear Optics Distributed Quantum Computing, Phy Rev. Lett., **95**, 030505 (2005).
9. RoyChowdhury, Sinha K. A., Mukhopadhyay S. - An all optical comparison scheme between two multi-bit data with optical nonlinear material, *Chinese Optics Lett.,* **6**, 693 (2008).
10. Dey S. Mukhopadhyay, S. - Approach of implementing phase encoded quantum square root of NOT gate, Electronics Letters, **53**, 1375 (2017).
11. Mukhopadhyay S. - Role of optics in super-fast information processing, Indian Journal of Physics 84, 1069 (2010).
12. Sun J.Lu, Liu S., F. - Adiabatically implementing quantum gates, Journal of Applied Physics, **115**, 224901 (2014).

13. Sarkar B., Mukhopadhyay S. -An all optical scheme for implementing an integrated Pauli's X, Y and Z quantum gates with optical switches, J. Opt., **46,** 143 (2017).
14. Pittman, T.B. Jacobs B.C., Franson J.D. - Demonstration of Nondeterministic Quantum Logic Operations Using Linear Optical Elements, Phy Rev Lett**., 88**, 257902(2002).
15. O'Brien J. L. Pryde, G. J.White, A. G. Ralph, T. C. etal - Demonstration of an all-optical quantum controlled-NOT gate, Nature, **426**, 264 (2003).
16. Garai,, S. K. Mukhopadhyay,, S. - A novel method of developing all-optical frequency encoded memory unit exploiting nonlinear switching character of semiconductor optical amplifiers, Optics and Laser Technology, **42**, 1122 (2010).
17. Ghosh B., Biswas S., Mukhopadhyay S. - A novel method of all-optical wavelength encoded logic and inhibitor operations with dibit representation technique, Optik**, 126(4),** 483 (2015).
18. Biswas S., Mukhopadhyay S. - An all optical approach for developing a system involving Kerr material based switches for cryptographic encoding of binary data depending on the input parity, Optik, **125**, 1954 (2014).

———————

INDIAN JOURNAL OF THEORETICAL PHYSICS, VOL 67, NOS. 1 & 2, 2019

Existance of Stable Lagrangian Point of A Cable-connected Satellites System under Several Influences of General Nature in Orbit

Sangam Kumar

Associate Professor, P. G. Department of Physics, L. S. College,
B. R. A. Bihar University, Muzaffarpur - 842001, Bihar, India.
E-mail:- kumarsangam.phy@gmail.com

[Abstract: Aim of the present work is to study the stability of Lagrangian point of motion of a system of two artificial satellites connected by a light, flexible, inextensible and non-conducting cable under the influence of solar radiation pressure, shadow of the earth, earth's magnetic field and air resistance. Case of circular orbit of centre of mass of the system is discussed. Here, one Lagrangian point exists when all the perturbations mentioned above act on the system simultaneously. Liapunov's theorem is applied to test the stability of the Lagrangian point. It is found that the Lagrangian point is unstable in the sense of Liapunov.]

Key-words: Cable-connected satellites, Lagrangian point, Stability Circular orbit, Liapunov's theorem

1. Introduction

Beletsky and Novikova1and Beletsky and Novoorebelskii[2] are the pioneer workers on the problems of two cable-connected artificial satellites. They studied the motion of a system of two cable-connected artificial satellites in the central gravitational field of force relative to its centre of mass. Singh and Demin[8] and Singh[9] investigated the problem in two and three dimensional cases. Kumar and Bhattacharya[3] studied about the stability of equilibrium position of two cable-connected satellites. Kumar and Srivastava[4] studied about evolutional and non-evolutional motion of a system of two cable-connected artificial satellites under some perturbative forces. Kumar and Kumar5 studied about equilibrium positions of a cable-connected satellites system under several influences. Kumar6 studied about libration points of cable-connected satellites system under the influence of solar radiation pressure, earth's magnetic field, shadow of the earth and air resistance in circular orbit.

Stability of Lagrangian point of motion of a system of two cable-connected artificial satellites under the influence of solar radiation pressure, shadow of the earth, earth's magnetic field and air resistance is discussed over here. The influence of the above mentioned perturbations on the system has been studied singly and by a combination of any two or three of them by various workers, but never conjointly all at a time. Therefore, these could not give a real picture of motion of the system. This fact has initiated the present research work. Shadow of the earth is taken to be cylindrical and the system is allowed to pass through the shadow beam. The cable connecting the two satellites is considered as light, flexible, inextensible and non-conducting string. Central attractive force of the earth will be the main force and all other forces, being small

enough are considered here as perturbing forces. The satellites are taken as charged material particles. Masses of the satellites are small. Distances between the satellites and other celestial bodies are very large. Therefore, gravitational forces of attraction between the satellites and other celestial bodies including the sun have been neglected.

2. Treatment of the problem

A set of equations for motion of the system in rotating frame of reference is written as Kumar[6]

$$X'' - 2Y' - 3X = \beta X - A\cos\ i + \left(\frac{B_1}{m_1} - \frac{B_2}{m_2}\right)\frac{\cos\in\cos\alpha\sin\theta_2}{\pi}$$

and

$$Y'' + 2Y' = \beta Y + \left(\frac{B_1}{m_1} - \frac{B_2}{m_2}\right)\frac{\cos\in\sin\alpha\sin\theta_2}{\pi} - f \quad \text{... (1)}$$

the condition of constraint is

$$X^2 + Y^2 \leq 1 \quad \text{... (2)}$$

Here,

$$A = \left(\frac{m_1}{m_1+m_2}\right)\left(\frac{Q_1}{m_1} - \frac{Q_2}{m_2}\right)\frac{\mu_E}{\sqrt{\mu\rho}}, \beta = \frac{p^3\lambda}{\mu}\left(\frac{m_1+m_2}{m_1m_2}\right)$$

$$\rho = \frac{1}{(1+e\cos V)}, f = \frac{a_1p^3}{\sqrt{\mu p}},$$

$$a_1 = \rho_a\dot{R}(c_2 - c_1)\left(\frac{m_1}{m_1+m_2}\right) \quad \text{... (3)}$$

m_1 and m_2 are masses of the two satellites. B_1 and B_2 are the absolute values of the forces due to the direct solar pressure on m_1 and m_2 respectively and are small Q_1 and Q_2 are the charges of the two satellites. μ_E is the magnitude of magnetic moment of the earth's dipole. p is the focal parameter. μ is the product of mass of the earth and gravitational

constant. λ is undermined Lagrange's multiplier. e is eccentricity of the orbit of the centre of mass. v is the true anomaly of the centre of mass of the system. $\in$ is inclination of the oscillatory plane of the masses m_1 and m_2 with the orbital plane of the centre of mass of the system. α is the inclination of the ray. γ is a shadow function which depends on the illumination of the system of satellites by the sun rays. If γ is equal to zero, then the system is affected by the shadow of the earth. If γ is equal to one, then the system is not within the said shadow. $\dot{R}$ is the first order time derivative of R. R is the modulus of position vector of the centre of mass of the system. c_1 and c_2 are the Ballistic co-efficient. ρ_a is the average density of the atmosphere. θ_2 is the angle between the axis of the cylindrical shadow beam and the line joining the centre of the earth and the end point of the orbit of the centre of mass within the earth's shadow, considering the positive direction towards the motion of the system. The system of two satellites is allowed to pass through the shadow beam during its motion. Prime denotes differentiation with respect to v.

Equations (1) do not contain the time explicitly. Therefore, Jacobean integral of the problem exists.

Multiplying the first and second equations of (1) by X' and Y' respectively, adding them and then integrating the final equation, Jacobean integral comes to the form

$$X'^2 + Y'^2 - 3X^2 = \beta - 2AX\cos i + \frac{2}{\pi}\left(\frac{B_1}{m_1} - \frac{B_2}{m_2}\right)$$

$$\cos \in \sin\theta_2 \,(X\cos\alpha + Y\sin\alpha) - 2fY + h \qquad \ldots(4)$$

θ_2 is taken to be constant. h is the constant of integration, called Jacobean constant.

3. Existance of Lagrangian points of the problem

Lagrangian points of the system are given by the constant values of the co-ordinates in the rotating frame of reference. Thus,

$X = X_0,$ and $Y = Y_0$ ... (5)

where X_0 and Y_0 are constant, give the Lagrangian points.

With the help of (5), the set of equations (1) may be written as

$$(3+\beta)X_0 = A\cos i - \left(\frac{B_1}{m_1} - \frac{B_2}{m_2}\right).\frac{\cos\in \cos\alpha \sin\theta_2}{\pi}$$

and

$$\beta Y_0 = f - \left(\frac{B_1}{m_1} - \frac{B_2}{m_2}\right).\frac{\cos\in \sin\alpha \sin\theta_2}{\pi} \quad \text{... (6)}$$

It is very difficult to obtain the solution of (6). Hence we are compelled to make our approaches with certain limitations. In addition to this, we are interested only to consider the maximum effect of the earth's shadow on the motion of the system.

The presence of perturbative term due to solar pressure indicates that none of the co-ordinates of the Lagrangian point may be taken to be zero unless $\left(\frac{B_1}{m_1} - \frac{B_2}{m_2}\right)$ or $\theta_2 = 0$. But these parameters cannot be zero. Hence in our further investigation $\in = 0$ and $\alpha = 0$.

By doing so, we get

$$(3+\beta)X_0 = A\cos i - \left(\frac{B_1}{m_1} - \frac{B_2}{m_2}\right).\frac{\sin\theta_2}{\pi}$$

and

$$\beta Y_0 = f \quad \text{...(7)}$$

All the two equations of (7) are independent of each other. Therefore, we get the Lagrangian point as

$$(X_0, Y_0) = \left[\frac{1}{(3+\beta)}\left\{A\cos i - \frac{1}{\pi}\left(\frac{B_1}{m_1} - \frac{B_2}{m_2}\right)\sin\theta_2\right\}, \frac{f}{\beta}\right] \quad \text{... (8)}$$

4. Stability of the Lagrangian point

I apply Liapunov's[7] theorem to test the stability of the Lagrangian point given by (8).

Let us assume that there are small variations in the co-ordinates at the given Lagrangian point denoted by δ_1 and δ_2, then

$$X = X_0 + \delta_1, \qquad Y = Y_0 + \delta_2$$
$$\therefore X' = \delta_1' \qquad Y' = \delta_2'$$
$$\therefore X'' = \delta_1'' \qquad Y'' = \delta_2'' \qquad \text{... (9)}$$

Using (9) in the equations (1), a set of variational equations comes to the form

$$\delta_1'' - 2\delta_2' - (X_0 + \delta_1)(3 + \beta) = \left(\frac{B_1}{m_1} - \frac{B_2}{m_2}\right)\frac{\sin\theta_2}{\pi} - A\cos i$$

and $\delta_1'' - 2\delta_2' - \beta(Y_0 + \delta_2) = -f$ ... (10)

where $\in = 0$ and $\alpha = 0$

As the original equations (1) admit Jacobean integral, the variational equations of motion (10) will also admit Jacobean integral.

Multiplying the first and second equations of (10) by $2\delta_1'$ and $2\delta_2'$ respectively, adding them and then integrating the final equation, Jacobean integral at the Lagrangian point becomes as

$$\delta_1'^2 + \delta_2'^2 + \delta_1^2(-3 - \beta) + \delta_2^2(-\beta) + \delta_1 \left[2\left\{A\cos i - (3 + \beta)X_0 - \left(\frac{B_1}{m_1} - \frac{B_2}{m_2}\right)\frac{\sin\theta_2}{\pi}\right\}\right] + \delta_2[2\{f - \beta Y_0\}] = h_1 \qquad \text{... (11)}$$

h_1 is the constant of integration at the Lagrangian point.

To test the stability in the sense of Liapunov[7], Jacobean integral is considered as Liapunov function $(\delta_1', \delta_2', \delta_1, \delta_2)$. Thus,

$$L(\delta_1', \delta_2',\ \delta_1,\ \delta_2) = \delta_1'^2 + \delta_2'^2 + \delta_1^2(-3-\beta) + \delta_2^2(-\beta) +$$
$$\delta_1\left[2\left\{A\cos i - (3+\beta)X_0 - \left(\frac{B_1}{m_1} - \frac{B_2}{m_2}\right)\frac{\sin\theta_2}{\pi}\right\}\right] + \delta_2[2\{f - \beta Y_0\}] \ldots (12)$$

5. Results and discussion

L is taken as Liapunov's function. As L is the integral of the system of variational equations (10), its differential taken along the trajectory of the system must vanish identically. Thus, only condition that the Lagrangian point be stable in the sense of Liapunov is that L must be positive definite. For making (12), a positive definite function, it is mandatory that the function does not have terms of first order in the variables whereas the terms of the second order must satisfy the Sylvester's conditions for positive definiteness of quadrative forms. Thus, the sufficient conditions for stability of the system at the Lagrangian point are

(i) $2\left\{A\cos i - (3+\beta)X_0 - \left(\frac{B_1}{m_1} - \frac{B_2}{m_2}\right)\frac{\sin\theta_2}{\pi}\right\} = 0$

(ii) $2\{f - \beta Y_0\} = 0$

(iii) $-(3+\beta) > 0$

and

(iv) $-\beta > 0$ ... (13)

6. Conclusion

For stability of the Lagrangian point in the sense of Liapunov, Jacobean integral at the Lagrangian point must be positive definite. This means that Liapunov's function must be positive definite. But in the present problem, Liapunov's function is not positive definite. It is based on the fact that all the four conditions for positive definiteness given by

(13) are not identically satisfied simultaneously. Therefore it is concluded that the Lagrangian point is unstable.

Acknowledgement

I am thankful to University Grants Commission, Kolkata for providing me the Research Project with Sanction Letter No. F. PSB-005/15-16, Dated 15.11.2016.

References

1. Beletsky V. V. and Novikova E. T.- Kosmicheskie Issledovania, **7 (6)**, pp. 377-384 (1969).
2. Beletsky V. V. and Novoorebelskii A. B. - Inst. Appl. Maths., Acad. Sci., U. S. S. R., Soviet Astronomy **17 (2)**, pp. 213-220 (1969).
3. Kumar S. and Bhattacharya P. K. – Proc. Workshop on Spa. Dyn. and Cel. Mech., Muz., India, **Eds. K. B. Bhatnagar and B. Ishwar**, pp. 71-74 (1995).
4. Kumar S. and Srivastava U. K. - Narosa publishing House, N. Delhi, Chennai, Mumbai, Kolkata, **Ed. B. Ishwar**, pp. 187-192 (2006).
5. Kumar S. and Kumar S – International Jour. Astro. Astrophy., **6**, pp. 288-292 (2016).
6. Kumar S. - Jour. Phy. Sci., **23**, pp. 165-170 (2018).
7. Liapunov A. M. - Sabrania Sachimeiviya Moscow (Russian), **2N**, pp. 327- 335 (1959).
8. Singh R. B. and Demin V. G. – Cel. Mech., **6**, pp. 268-277 (1972).
9. Singh R. B. – Astronau. Acta, **18**, pp. 301-308 (1973).

———————

INFORMATION TO AUTHORS

Manuscripts should represent results of original works on theoretical physics or experimental physics with theoretical background or on applied mathematics. Letters to the Editor and Review articles in emerging areas are also published. Submission of the manuscript will be deemed to imply that it has not been published previously and is not under consideration for publication elsewhere (either partly or wholly) and further that, if accepted, it will not be published elsewhere. It is the right of the Editorial Board to accept or to reject the paper after taking into consideration the opinions of the references.

Manuscripts may be submitted in pdf/MS word format to **admin@citphy.org or susil_vcsarkar@yahoo.co.in** Online submission of the paper through our **website: www.citphy.org** is also accepted. The file should be prepared with 2.5 cm margin on all sides and a line spacing of 1.5.

The title of the paper should be short and self-explanatory. All the papers must have an abstract of not more than 200 words, the abstract page must not be a part of the main file. Abstract should be self-contained. It should be clear, concise and informative giving the scope of the research and significant results reported in the paper. Below the abstract four to six key words must be provided for indexing and information retrieval.

The main file should be divided into sections (and sub-sections, if necessary) starting preferably with introduction and ending with conclusion. Displayed formula must be clearly typed (with symbols defined) each on a separate line and well-separated from the adjacent text. Equations should be numbered with on the right-hand side consecutively throughout the text. Figures and Tables with captions should be numbered in Arabic numerals in the order of occurrence in the text and these should be embedded at appropriate places in the text. Associated symbols must invariably follow SI practice.

References should be cited in the text by the Arabic numerals as superscript. All the references to the published papers should be numbered serially by Arabic numerals and given at the end of the paper. Each reference should include the author's name, title, abbreviated name of the journal, volume number, year of publication, page numbers as in the simple citation given below :

For Periodicals : Sen, N. R. - On decay of energy spectrum of Isotopic Turbulence, 1. Appl. Phys. **28,** No. 10, 109-110 (1999).

1. Mikhilin, S. G. - Integral Equations, Pergamon Press, New York (1964).
2. Hinze, A. K. - Turbulence Study of Distributed Turbulent Boundary Layer Flow, Ph. D, Thesis, Rorke University (1970).

The corresponding author will receive page proof, typically as a pdf file. The proof should be checked carefully and returned to the editorial office within two or three days. Corrections to the proof should be restricted to printing errors and made according to standard practice. At this stage any modifications (if any) made in the text should be highlighted.

To support the cost of publication of the journal, the authors (or their Institutions) are requested to pay publication charge ₹ 200/- per printed page for authors of Indian Institutes and US$ 20 for others. Publication charges to be sent directly to **CALCUTTA INSTITUTE OF THEORETICAL PHYSICS, 'BIGNAN KUTIR', 4/1 MOHAN BAGAN LANE, KOLKATA-700004, INDIA.**

A pdf of the final publisher's version of the paper will be sent to the corresponding author.

All communications are to be sent to the Secretary, Calcutta Institute of Theoretical Physics, 'Bignan Kutir', 4/1, Mohan Bagan Lane, Kolkata-700004, India. E-mail: susil_vcsarkar@yahoo.co.in

For details please visit our website www.citphy.org

INDIAN JOURNAL OF THEORETICAL PHYSICS

CALCUTTA INSTITUTE OF THEORETICAL PHYSICS

(Formerly, Institute of Theoretical Physics)

[Established in 1953 by Late Prof. K. C. Kar, D. Sc.]

PUBLICATIONS
OF
CALCUTTA INSTITUTE OF THEORETICAL PHYSICS
"BIGNAN KUTIR"
4/1, Mohan Bagan Lane, Kolkata-700 004, India
Phone : +91-33-25555726

INDIAN JOURNAL OF THEORETICAL PHYSICS (ISSN : 0019-5693)
Research Journal containing Original Papers, Review Articles and Letters to the Editor is published quarterly in March, June, September and December and circulated all over the world.

Subscription Rates
₹ 1500 per volume (for Bonafide Indian Party)
US$ 350 (for Foreign Party)

Back Volume Rates
₹ 1500 per volume (for Bonafide Indian Party)
US$ 350 per volume or Equivalent Pounds per volume

Books Written by Prof. K. C. Kar, D. Sc.

- **INTRODUCTION TO THEORETICAL PHYSICS [Vol. I and Vol. II (Acoustics)]** Useful to students of higher physics
  Price :₹ 60 or US $ 10 per volume
- **WAVE STATISTICS : Its principles and Applications [Vol. I and Vol. II]** Useful to Post Graduate and Research students
  Price :₹ 80 or US $ 12
- **STATISTICAL MECHANICS : PRINCIPLES AND APPLICATIONS [Vol. I and Vol. II]** Useful to Advanced students of theoretical Physics
  Price :₹ 120 or US $ 15
- **A NEW APPROACH TO THE THEORY OFRELATIVITY [Vol. I and Vol. II]** Useful to Post Graduate and advanced students
  Price :₹ 50 or US $ 8

Order may be sent directly to Calcutta Institute of Theoretical Physics
"BignanKutir", 4/1, Mohan Bagan Lane, Kolkata-700 004, India